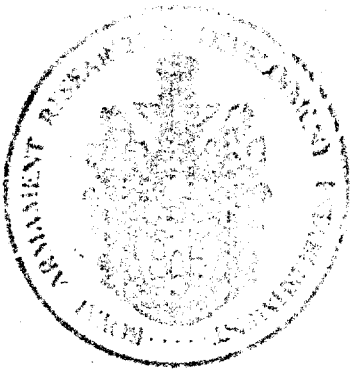

(4)

MINISTRY OF DEFENCE

ROYAL

ARMAMENT RESEARCH AND DEVELOPMENT ESTABLISHMENT

REPORT 4/82

Investigation of Residual Stresses in a Hot Cured Glass Fibre Reinforced Epoxy Resin Composite

M.J. Hinton

MINISTRY OF DEFENCE

ROYAL ARMAMENT RESEARCH AND DEVELOPMENT ESTABLISHMENT

REPORT 4/82

Investigation of Residual Stresses in a Hot Cured Glass Fibre Reinforced Epoxy Resin Composite

M J Hinton MSc

Summary

Basic lamina elastic constants and thermal expansion coefficients have been determined for an 'E' glass fibre reinforced epoxy resin system over a range of fibre contents. These have been used as input data to a theoretical model which predicts laminate residual strains and stresses. Residual strains have also been measured experimentally. Theory and experiment were in good agreement indicating a stress-free temperature comparable to the heat deflection temperature of the resin. It is shown that in some cases residual stresses can be significant percentages of the ultimate strength of the lamina and must be allowed for in design.

CONTENTS

A

1 INTRODUCTION

The recent growth in the use of fibre reinforced composite materials for primary structures has stimulated the development of more accurate methods of predicting their mechanical performance. Initial design codes were very conservative, often incorporating 'plastics factors' to allow for the lack of experience and confidence in composite materials. If the behaviour of these materials were better understood and the real behaviour could be more accurately modelled in design codes, this margin of over-design could be reduced and better advantage taken of the high specific strength and stiffness of these materials.

Initial work at RARDE on balanced symmetric angle-ply GRP tubes (Ref 1) showed that good agreement could be obtained between elastic properties measured experimentally and properties predicted by Continuum Theory. Continuum Theory is a method of mathematically assembling the mechanical properties of a general laminate from the mechanical properties of blocks of suitably oriented unidirectional laminae (Ref 2). Current work at RARDE is aimed at developing a Continuum Theory-based computer model for predicting the mechanical properties of a general reinforced plastic laminate under complex loading (Ref 3). Experimental verification of this model under a variety of loading conditions is clearly essential in order to establish confidence in its use.

Little work has been reported on the magnitudes of residual curing stresses and their effect on the performance of laminates under Service conditions. It is known that laminates of certain lay-up configurations can be broken during fabrication by curing stresses alone. In less severe cases, whilst the laminate may still be intact after fabrication, subsequent loading under Service conditions may lead to premature failure if the residual and service stresses are additive. For accurate design work it is therefore essential to take residual curing stresses into account.

The objectives of the present study were:

a) to determine the data necessary for a theoretical analysis capable of giving the magnitude of residual stresses in a general laminate,

b) using a suitable laminate, to measure the residual curing strains experimentally, and to compare these with the theoretical values,

c) to determine the implications for design methods.

2 CHOICE OF MATERIALS

A wide range of fibres and resin systems is readily available. However, in order to limit the number of variables, a standard resin/glass system has been adopted for all modelling studies at RARDE. The materials used were:

a) Silenka 051L, 1200 tex, 'E' glass fibre rovings

b) Ciba-Geigy epoxy resin MY750, hardener HY917 and accelerator DY063 mixed in the proportions 100:85:2 by weight.

The cure cycle was 2 hours at 90°C followed by 1 hour at 130°C and finally 1.5 hours at 150°C. Differential scanning calorimetry has shown that this cycle yields a fully cured resin system.

The specific reasons for selecting the above system are given elsewhere (Ref 4).

3 MATERIALS DATA REQUIRED FOR THEORETICAL MODELLING

Accurate measurement of the elastic properties and thermal expansion coefficients of representative unidirectional laminae is fundamental to this type of analysis. The properties required are:

E_L	Longitudinal tensile modulus
E_T	Transverse tensile modulus
μ_{LT}	Major Poisson's Ratio
μ_{TL}	Minor Poisson's Ratio
G_{LT}	In-plane shear modulus
α_L	Longitudinal coefficient of thermal expansion
α_T	Transverse coefficient of thermal expansion

Composites of most interest for high performance applications have a fibre content of between 0.5 and 0.7 parts by volume (V_F). The properties outlined above are therefore required for all composites in the range V_F=0.5 to 0.7.

There are problems in trying to extrapolate data measured at one fibre content to a different content. This is discussed elsewhere (Ref 1). In order to avoid extrapolation, μ_{LT}, μ_{TL}, E_T, E_L, α_L and α_T were measured on flat rectangular specimens, each with a different fibre content. Hoop wound cylinders loaded in torsion were used to determine G_{LT}.

4 SPECIMEN MANUFACTURE

4.1 Flat Rectangular Tensile Specimens

Flat, unidirectional plates of the chosen glass/epoxy system were manufactured using a process developed at AERE (Ref 5). A filament winding machine was used to lay down a circumferential pattern onto a flat plate mandrel. After a sufficient thickness had built up, the mandrel was heated to the resin gel temperature (90°C) in an oven, and held at that temperature for approximately 2 hours. The mandrel was then air cooled to room temperature, and the winding pattern cut through at the edges of the flat plate. The two halves of the winding pattern could then be lifted

from the mandrel and, because the resin had gelled, the laminate could be easily handled. Each half was used to make a separate plate by placing it in a rectangular leaky mould which was held closed (suitably shimmed) by G-clamps. The assembly was heated in an oven to complete the composite cure cycle. As curing proceeded, a periodic check was made to ensure that the G-clamps were holding the mould closed onto the shims, which ensured uniform plate thickness. On completion of the curing cycle, the mould was air cooled to room temperature, the G-clamps removed and the flat plate extracted.

The as-moulded plate dimensions were approximately 1mm x 250mm x 250mm. Tensile specimens 25mm x 250mm were cut from the plates using a diamond impregnated wheel. Two types of specimen were cut, one along the fibre direction (to give E_L and μ_{LT}), and one transverse to the fibre direction (to give E_T and μ_{TL}). Aluminium tabs were bonded to the ends of the specimens to prevent grip damage on testing, and strain gauges (1 longitudinal and 1 transverse) were mounted in the centre using cyanoacrylate adhesive. TML gauges types FLA-10-11 and FLA-6-11 were used throughout.

4.2 Hoop Wound Cylindrical Specimens

These specimens were manufactured by the filament winding process (Ref 6). A circumferential pattern was used to lay an 8mm bandwidth onto a 51mm diameter aluminium mandrel. The specimens were reinforced at the ends by using the winding pattern shown schematically in Figure 1. This ensured that the specimen would fail in the centre section.

In order to transmit the torsional load to the GRP specimen, aluminium plugs were bonded into the ends. A bond length of 35mm was found to be sufficient. The joint was manufactured as follows:

A 51mm diameter 'O' ring was positioned 35mm along the plug to be bonded. This prevented leakage of adhesive from the joint during curing. The surfaces to be bonded were lightly abraded and degreased, and the adhesive was spread evenly over both surfaces. The plug was then positioned in the tube so that the 'O' ring was in firm contact with the end face of the tube. The assembly was supported in a vertical position using a laboratory stand and clamps. The selected adhesive, Araldite AW134B/HY994, required a 3 hour cure at 60°C and this was carried out in an air circulating oven. Bonding was completed at one end before the second plug, which contained a vent hole, was inserted.

In preliminary torsion tests failures occurred at the adhesive/GRP interface. Subsequently, the GRP surface was thoroughly abraded and freed from any mould release agent remaining from the filament winding process. This process change prevented interface failures during further tests where shear failure within the gauge length of the GRP was achieved.

On completion of bonding a 0°/90° TML strain gauge rosette (type FCA-6-11) was bonded centrally to each specimen. The gauge axes were aligned at ±45° to the longitudinal axis of the tube.

5 TEST PROCEDURE

5.1 Tensile Tests

The specimens were loaded in an Instron 1193 tensile testing machine, using wedge grips and a constant crosshead speed of 1mm/minute. The strain gauges were connected independently in quarter bridge configuration to two Peekel Model CA300 strain gauge bridges. Each bridge output was connected to the separate channels of an X-Y_1Y_2 recorder, so that load vs longitudinal strain and load vs transverse strain could be plotted simultaneously on the same graph throughout the test. The specimens were loaded to 0.2% strain for the longitudinal samples, and 0.1% strain for the transverse samples, which ensured that no damage occurred to the specimens. Linear load-strain graphs were obtained over these ranges, and the moduli and Poisson's ratio were obtained from the slopes of lines drawn through the origin to the maximum strain point.

5.2 Thermal Tests

The specimens made for the tensile tests were also used to determine the thermal expansion coefficients of unidirectional laminae. The test method adopted is described fully in Reference 7. It relies on the detection of the differential expansion between GRP and a reference material (steel) by strain gauges connected in half bridge configuration. By using two bridges and two reference gauges connected to an X-Y_1Y_2 recorder, both α_L and α_T were measured simultaneously on the same sample. For reasons described in Reference 7, a more accurate answer can be obtained by carrying out the test between room temperature and -50°C. These conditions were used in the present work. The temperature dependence of α_L and α_T is discussed later (Section 8.6).

5.3 Torsion Tests

The specimens were loaded in a Mayes 250kN-m capacity servohydraulic torsion machine. Adaptors were designed so that the grips supplied with the machine for torsion testing British Standard metal specimens could be used to load the GRP cylinders. The complete assembl is shown in Figure 2. Before testing was started, the two strain gauge were connected in full bridge configuration with two dummy gauges to a Peekel Model CA300 strain gauge bridge. When the active gauges were connected in adjacent arms of the bridge, the bridge measured shear strain directly. An X-Y plotter was used to display torque vs shear strain as the test proceeded. The loading rate was manually controlled, the time to failure being approximately 30 seconds.

5.4 Determination of Fibre Content

The resin burnoff technique defined by BS2782 Method 107J (1970) was used to measure the glass weight fraction. From this the fibre volume fraction was calculated. The density of 'E' glass is 2.55g/ml and that of epoxy resin is 1.18g/ml. Care was taken with the tensile samples to remove all traces of the strain gauges and wiring tabs so that the centre portion could be used in the burnoff test.

6 RESULTS

6.1 Tensile Samples

Tables 1 and 2 summarise the experimental results. The following equations were used to calculate theoretical values of E_L, E_T, μ_{LT} and μ_{TL}. Subscripts F and M refer to fibre and matrix properties respectively.

a) E_L prediction by the Modified Law of Mixtures (Ref 8)

$$E_L = V_F E_F + V_M E_M^1 \tag{1}$$

where $$E_M^1 = \frac{E_M}{(1-2\mu_M^2)}$$

b) E_T prediction using the expression developed by Tsai (Ref 9)

$$E_T = 2[1-\mu_F+(\mu_F-\mu_M)V_M]\left[[1-C]\ \frac{K_F(2K_M+G_M)-G_M(K_F-K_M)V_M}{(2K_M+G_M)+2(K_F-K_M)V_M}\right.$$

$$\left.+C\ \frac{K_F(2K_M+G_F)+G_F(K_M-K_F)V_M}{(2K_M+G_F)-2(K_M-K_F)V_M}\right] \tag{2}$$

where $K_F = E_F/2(1-\mu_F)$

$K_M = E_M/2(1-\mu_M)$

$G_F = E_F/2(1+\mu_F)$

$G_M = E_M/2(1+\mu_M)$

and C is a contiguity factor, ranging from C=1 for filaments in contact to C=0 for isolated filaments.

c) μ_{LT} prediction by the Law of Mixtures (Ref 8)

$$\mu_{LT} = V_F\mu_F + V_M\mu_M \tag{3}$$

d) μ_{TL} prediction by the Reciprocal Theorem (Ref 2)

$$\frac{\mu_{TL}}{\mu_{LT}} = \frac{E_T}{E_L} \tag{4}$$

Where values of μ_{LT}, E_T and E_L have previously been calculated from theory using equations 1 to 3, this expression can be used to calculate μ_{TL}.

e) α_L prediction (Ref 7)

$$\alpha_L = \alpha_F + (\alpha_M - \alpha_F) \frac{(1-V_F)E_M}{(1-V_F)E_M + V_F E_F} \quad (5)$$

f) α_T prediction (Ref 7)

$$\alpha_T = \alpha_F V_F + \alpha_M(1-V_F) \quad (6)$$

The following values of elastic constants for fibre and matrix were used to evaluate equations 1 to 6. These values were obtained during previous work (references in parentheses).

Matrix Properties:

$E_M = 3.352$ GPa (Ref 1)

$\mu_M = 0.351$ (Ref 1)

$\alpha_M = 58.5$ μstrain/°C (Ref 7)

Fibre Properties:

$E_F = 73.0$ GPa (Ref 8,9)

$\mu_F = 0.23$ (Ref 8,9)

$\alpha_F = 4.9$ μstrain/°C (Ref 10)

There seem to be substantial variations in values quoted for μ_F in the literature. Experimentally this is a difficult property to measure. Broutman and Krock (Ref 10) have summarised the work in this area, showing values ranging from 0.18±0.02 (Ref 11) to 0.34±0.07 (Ref 12). The glass manufacturers, Silenka, indicate a range of values from 0.18 to 0.25 in their own literature survey (Ref 13). As part of a contract sponsored by RARDE at Surrey University, Manders and Bader (Ref 14) have reported values for μ_F of 0.37. These were preliminary results obtained by using a light scattering technique. For the work reported here it was decided to use a value of μ_F=0.23.

Tables 3 and 4 show the theoretical predictions for elastic constants and thermal expansion coefficients. Figures 3 to 8 are graphs of experimental vs theoretical results. Figure 3 shows that agreement between experimental results and the modified Law of Mixtures is very good. Figure 4 shows that the Tsai equation fits the experimental results reasonably well for contiguity factors (degree of fibre to fibre contact) of 0.4 to 0.5. A single value of 0.45 would seem appropriate for further predictions. Figures 5 and 6 showing the major and minor Poisson's Ratios indicate a large scatter in the experimental results. Nevertheless, the theoretical curves do pass between the experimental points, showing some agreement. Figure 7 indicates that the theoretical curve for α_L forms a lower boundary to the experimental results. A linear expression was fitted to the data giving a correlation coefficient of 0.78:

$$\alpha_L = 19.6 - 18.4V_F \quad (7)$$

Figure 8 shows that prediction of α_T is in quite good agreement with the experimental results. A better fit was obtained with a linear expression, giving a correlation coefficient of 0.84:

$$\alpha_T = 71.3 - 74.9V_F \quad (8)$$

6.2 Torsion Samples

Figure 9 shows the stress/strain curves from the eleven samples tested. A fourth order polynomial gave the best fit to the data:

$$\tau = -0.484\gamma^4 + 6.281\gamma^3 - 30.966\gamma^2 + 72.584\gamma + 0.031 \quad (9)$$

where τ = shear stress (MPa)

γ = shear strain (%)

Table 5 gives the test data at failure of the specimens. It should be noted that the glass content did not vary significantly from specimen to specimen.

6.3 Summary of Results

The equations shown below result from the substitution of the values for fibre and matrix elastic properties given in Section 6.1 into the theoretical equations justified by Figures 3 to 6. These can be used to predict unidirectional lamina elastic constants for fibre volume fractions between 0.50 and 0.70.

$$E_L = 73.0V_F + 4.448(1-V_F) \quad (10)$$

$$E_T = [1.298+0.242V_F]\left[\frac{136.39+30.59V_F}{96.0-89.64V_F} + \frac{598.4V_F+144.64}{124.48-89.64V_F}\right] \quad (11)$$

$$\mu_{LT} = 0.23V_F + 0.351(1-V_F) \quad (12)$$

$$\mu_{TL} = \frac{E_T}{E_L} \times \mu_{LT} \quad (13)$$

Thermal expansion coefficients can be predicted for unidirectional laminae with fibre volume fractions between 0.50 and 0.70 using the equations below, which were obtained from the best fits shown in Figures 7 and 8.

$$\alpha_L = 19.6 - 18.4V_F \quad (7)$$

$$\alpha_T = 71.3 - 74.9V_F \quad (8)$$

Shear stiffness behaviour was markedly non-linear for this glass/resin system. Stress/strain curves were not obtained for laminae covering the range 0.50 to 0.70. The samples tested were closely grouped with an average glass content of 61% by volume, and their shear stress/strain behaviour can be represented by:

$$\tau = -0.484\gamma^4 + 6.281\gamma^3 - 30.966\gamma^2 + 72.584\gamma + 0.031 \qquad (9)$$

where τ = shear stress (MPa)

γ = shear strain (%)

When equations 1 to 6 are used the predicted unidirectional lamina elastic constants and thermal expansion coefficients for fibre volume fractions between 0.50 and 0.70 are as follows:

V_F	E_L (GPa)	E_T (GPa)	μ_{LT}	μ_{TL}	α_L $\mu\varepsilon/°C$	α_T $\mu\varepsilon/°C$
0.5	38.72	12.105	0.290	0.0907	10.40	33.85
0.55	42.15	13.680	0.283	0.092	9.48	30.11
0.60	45.58	15.565	0.278	0.0945	8.56	26.36
0.65	49.01	17.750	0.271	0.098	7.64	22.62
0.70	52.43	20.320	0.266	0.1035	6.72	18.87

7 ANALYSIS OF THERMAL STRESS BY LAMINATE THEORY

7.1 Definition of Terms

A full derivation of the equations used to evaluate the residual curing stresses in a laminated plate is given in Reference 2. The computer code developed in Reference 3 was used in this report for the theoretical analysis (see Section 8.5). Some of the terms and definitions required are given below.

a) Two sets of axes are normally required to define the mechanical properties of an angle-ply laminate. The 'LT' axes are oriented parallel and perpendicular to the fibre direction of each lamina, and they are called the 'natural' axes. The 'XY' axes are usually fixed along lines of symmetry of the component. For a tube for instance the hoop and axial directions are usually chosen as XY axes. The angle between the 'LT' and 'XY' axes is the transformation angle θ. The sign convention is defined in Reference 3.

b) The stiffness matrix of a unidirectional composite lamina in natural axes is defined as:

$$[C]_{LT} = \begin{bmatrix} E_L/(1-\mu_{LT}\mu_{TL}) & E_L\mu_{TL}/(1-\mu_{LT}\mu_{TL}) & 0 \\ E_L\mu_{TL}/(1-\mu_{LT}\mu_{TL}) & E_T/(1-\mu_{LT}\mu_{TL}) & 0 \\ 0 & 0 & G_{LT} \end{bmatrix} \qquad (14)$$

c) Mechanical properties in 'LT' coordinates can be transformed mathematically to give properties in 'XY' directions. The transformation matrix is:

$$[T] = \begin{bmatrix} M^2 & N^2 & -2MN \\ N^2 & M^2 & 2MN \\ MN & -MN & M^2-N^2 \end{bmatrix} \qquad (15)$$

where $M = \cos\theta$

$N = \sin\theta$

d) Transforming a lamina stiffness matrix requires an expression as follows:

$$[C]_{XY} = [T]^{-1} [C]_{LT}[T] \qquad (16)$$

e) For a laminated anisotropic plate element with applied in-plane loads N_X, N_Y and N_{XY} and moments M_X, M_Y and M_{XY} the reference surface strains and plate change of curvature/twists are related by:

$$\begin{bmatrix} N \\ \cdots \\ M \end{bmatrix}_{XY} = \begin{bmatrix} A & -B \\ \cdots & \cdots \\ B & -D \end{bmatrix}_{XY} \begin{bmatrix} \epsilon_o \\ \chi \end{bmatrix}_{XY} \qquad (17)$$

The middle surface of the plate is normally chosen as the reference surface though this is not essential. The distance from each lamina interface to the reference surface is denoted by H_K, so that the Kth lamina lies between interfaces at H_K and H_{K-1}. The [A] [B] and [D] matrices are then assembled as follows:

$$A_{IJ} = \sum_{k=1}^{N} [C_{IJ}]_{XY}^{K} (H_K - H_{K-1}) \qquad (18)$$

$$B_{IJ} = \frac{1}{2} \sum_{k=1}^{N} [C_{IJ}]_{XY}^{K} (H_K^2 - H_{K-1}^2) \qquad (19)$$

$$D_{IJ} = \frac{1}{3} \sum_{k=1}^{N} [C_{IJ}]_{XY}^{K} (H_K^3 - H_{K-1}^3) \qquad (20)$$

A_{IJ} refers to the term in the Ith row and Jth column of the [A] matrix.

The summation is carried out through the laminate thickness from K=1 to N, where K is the lamina number and N is the number of laminae forming the laminate.

$[C_{IJ}]^K_{XY}$ refers to the term in the Ith row and Jth column of the reduced stiffness matrix $[C]_{XY}$ containing properties appropriate to the Kth layer.

f) In order to calculate plate deformations due to a given applied load, equation 17 must be fully inverted. The final equation becomes:

$$\begin{bmatrix} \varepsilon_o \\ \cdots \\ \chi \end{bmatrix}_{XY} = \begin{bmatrix} a - bd^{-1}\, b^T & bd^{-1} \\ \cdots\cdots\cdots & \cdots\cdots \\ -d^{-1}\, b & d^{-1} \end{bmatrix}_{XY} \begin{bmatrix} N \\ \cdots \\ M \end{bmatrix}_{XY} \qquad (21)$$

The 3x3 matrices [a] [b] and [d] are defined as follows:

$$[a] = [A]^{-1} \qquad (22)$$

$$[b] = [A]^{-1}[B] \qquad (23)$$

$$[d] = [B][A]^{-1}[B] - [D] \qquad (24)$$

g) The strain on any surface through the laminate, other than the reference surface, can be obtained from:

$$[\varepsilon_z]_{XY} = [\varepsilon_o]_{XY} - z[\chi]_{XY} \qquad (25)$$

where $[\varepsilon_z]$ contains strains in XY coordinates of a surface at distance z above the reference surface.

h) Stresses in the Kth layer of a laminate can be obtained by substituting the appropriate value (either H_K or H_{K-1}) into equation 28 and using:

$$[\sigma]^K_{XY} = [C]^K_{XY}\ [\varepsilon]^K_{XY} \qquad (26)$$

i) Transformation of stresses or strains from 'XY' to 'LT' axes can be achieved using:

$$[\sigma]^K_{LT} = [T]^K\ [\sigma]^K_{XY}$$

$$[\varepsilon]^K_{LT} = [T]^K\ [\varepsilon]^K_{XY} \qquad (27)$$

7.2 Thermally Induced Stresses in a Laminated Plate

Hot cured laminated plates manufactured using epoxy resins are typically gelled at 80°C and post cured at temperatures greater than 100°C. Assuming that the operating condition is room temperature (say 20°C), a significant temperature difference exists between this and the stress-free temperature (somewhere near the gel temperature) of the plate. If each layer were free to deform independently, the temperature difference would cause simple thermal strains in each layer.

The analysis first assumes that 'thermal forces and moments' act on each layer causing thermal strains. The magnitude of these forces and moments can be calculated using the following set of equations, derived in Reference 2.

$$N_X^T = \sum_{K=1}^{N} \left[[C_{11}]_{XY}^K \alpha_X^K + [C_{12}]_{XY}^K \alpha_Y^K + [C_{13}]_{XY}^K \alpha_{XY}^K \right] (H_K - H_{K-1})\Delta T$$

$$N_Y^T = \sum_{K=1}^{N} \left[[C_{12}]_{XY}^K \alpha_X^K + [C_{22}]_{XY}^K \alpha_Y^K + [C_{23}]_{XY}^K \alpha_{XY}^K \right] (H_K - H_{K-1})\Delta T$$

$$N_{XY}^T = \sum_{K=1}^{N} \left[[C_{13}]_{XY}^K \alpha_X^K + [C_{23}]_{XY}^K \alpha_Y^K + [C_{33}]_{XY}^K \alpha_{XY}^K \right] (H_K - H_{K-1})\Delta T \qquad (28)$$

$$M_X^T = \sum_{K=1}^{N} \frac{1}{2} \left[[C_{11}]_{XY}^K \alpha_X^K + [C_{12}]_{XY}^K \alpha_Y^K + [C_{13}]_{XY}^K \alpha_{XY}^K \right] (H_K^2 - H_{K-1}^2)\Delta T$$

$$M_Y^T = \sum_{K=1}^{N} \frac{1}{2} \left[[C_{12}]_{XY}^K \alpha_X^K + [C_{22}]_{XY}^K \alpha_Y^K + [C_{23}]_{XY}^K \alpha_{XY}^K \right] (H_K^2 - H_{K-1}^2)\Delta T$$

$$M_{XY}^T = \sum_{K=1}^{N} \frac{1}{2} \left[[C_{13}]_{XY}^K \alpha_X^K + [C_{23}]_{XY}^K \alpha_Y^K + [C_{33}]_{XY}^K \alpha_{XY}^K \right] (H_K^2 - H_{K-1}^2)\Delta T$$

The forces and moments acting on each layer are summed through the thickness of the laminate. Thus N_X^T, N_Y^T and N_{XY}^T are the thermal forces, and M_X^T, M_Y^T and M_{XY}^T are the thermal moments acting on the laminate as a whole and where:

ΔT is the temperature difference between the operating temperature and the stress free temperature. For hot cure systems this is a negative quantity.

α_X^K is the coefficient of thermal expansion of the material in the Kth layer, measured in the X direction.

α_Y^K is the coefficient of thermal expansion of the material in the Kth layer, measured in the Y direction.

α_{XY}^K is a cross coefficient of thermal expansion, measured in the XY plane (analogous to a shear strain.)

The thermal expansion coefficients acting in the X and Y directions of a layer can be calculated from their coefficients in natural 'LT' axes by transformation:

$$[\alpha]_{XY}^K = [T]^K [\alpha]_{LT}^K \qquad (29)$$

The laminated plate equation 21, can now be used to determine the overall deformation due to the thermal forces and moments:

$$\text{ie} \quad \begin{bmatrix} \varepsilon_o \\ \\ \chi \end{bmatrix}_{XY}^{THERMAL} = \begin{bmatrix} a-bd^{-1}b^T & bd^{-1} \\ \\ -d^{-1}b^T & d^{-1} \end{bmatrix}_{XY} \begin{bmatrix} N \\ \\ M \end{bmatrix}_{XY}^{THERMAL} \tag{30}$$

The thermal strains in each lamina can be calculated using equation 25:

$$[\varepsilon_z]_{XY}^{THERMAL} = [\varepsilon_o]_{XY}^{THERMAL} - z[\chi]_{XY}^{THERMAL} \tag{31}$$

Transforming to natural axes gives:

$$[\varepsilon_z]_{LT}^{THERMAL} = [T][\varepsilon_z]_{XY}^{THERMAL} \tag{32}$$

The strain state in each lamina, calculated from equations 30 to 32, takes into account the restraining effects of adjoining laminae which ensures equilibrium through the laminate. However, if the laminae were all separated, their 'free' deformation would be governed by simple thermal expansion:

$$\text{ie} \quad \begin{bmatrix} \varepsilon_L \\ \varepsilon_T \\ \gamma_{LT} \end{bmatrix}_{LT}^{FREE} = \begin{bmatrix} \alpha_L \cdot \Delta T \\ \alpha_T \cdot \Delta T \\ 0 \end{bmatrix}_{LT} \tag{33}$$

The difference between the equilibrium and free strain state gives rise to mechanical strains, which then result in residual stresses:

$$\text{ie} \quad \begin{bmatrix} \varepsilon_L \\ \varepsilon_T \\ \gamma_{LT} \end{bmatrix}^{MECHANICAL} = \begin{bmatrix} \varepsilon_L \\ \varepsilon_T \\ \gamma_{LT} \end{bmatrix}^{THERMAL} - \begin{bmatrix} \alpha_L \cdot \Delta T \\ \alpha_T \cdot \Delta T \\ 0 \end{bmatrix}^{FREE} \tag{34}$$

The residual stress state in the lamina can be obtained from equation 34 by multiplying the LHS by the appropriate lamina stiffness matrix:

$$\text{ie} \quad [\sigma]^{\text{RESIDUAL}}_{LT} = [C]_{LT}\,[\varepsilon]^{\text{MECHANICAL}}_{LT} \tag{35}$$

To summarise, the overall deformation of a laminate due to thermal contraction or expansion can be obtained from equation 30. Equation 34 is required to evaluate the mechanical residual strains in any one lamina. The residual stress state in any one lamina can be found from equation 35.

The computer code developed in Reference 3 analyses the residual stress state in a given laminate by means of the equations discussed above. The program output includes the overall laminate deformation (equation 30), the mechanically induced residual strains in each lamina (equation 34) and the mechanically induced residual stress in each lamina (equation 35). Options for restraining the plate deformations during curing are available in the program, though this is not discussed here.

8 EXPERIMENTAL TECHNIQUE FOR MEASURING RESIDUAL THERMAL STRAIN IN A LAMINATE

8.1 Choice of Specimen

The simplest specimen geometry consists of one lamina at 0° and one at 90° to an arbitrary XY axis system. This is the worst case of asymmetry possible in terms of thermal expansion coefficients, being analogous to a bimetallic strip. With this configuration thermal forces lead to pure bending of the laminate, which becomes curved (in both X and Y directions). The radius of curvature (R) can be measured and the curvature (χ) calculated, since by definition:

$$\chi = \frac{1}{R} \tag{36}$$

Choosing a 0°/90° configuration has a further advantage in that deformations along the X axis are the mirror-images of deformations along the Y axis. Thus a check can be made to ensure that the 0° and 90° fibre directions coincide with the chosen X and Y directions (if they do not, deformations along the X axis will differ from those along the Y axis).

The validity of the laminate analysis outlined in Section 7 can be tested by comparing the theoretical values of χ (determined by evaluation of equation 26) with the experimentally measured values of χ.

8.2 Specimen Manufacture

The technique outlined in Section 4.1 was used. The flat plate mandrel was designed so that it could be rotated by 90° after completion of one or more layers. Thus a 0°/90° plate could be wound in one sequence. Gelling and curing were carried out in the same way as for the unidirectional plates.

On completion of cure, as soon as the mould constraints were removed, the laminates took on a curved shape.

Two sets of laminates were made, one with 0°/90° sequence (2 laminae), and the other with 0°/0°/90°/90° sequence (4 laminae). An as-moulded laminate was typically 250mm x 250mm. The radius of curvature (R) was measured along the X and Y axes (0° and 90° direction) through the centre of the plate. A straight edge and a depth gauge were used for this purpose and R was calculated by means of the geometric relationship shown in Figure 10. To minimise the problem of having a compound curvature acting on the plate, the plates were cut into 25mm x 250mm strips. Radius of curvature could thus be determined with C=250mm (see Fig 10).

If the radii of curvature along X and Y were significantly different, the plate was rejected since only imperfections could cause this. If the radii were similar, the plate was considered acceptable.

8.3 Test Procedure

The radius of curvature of each strip was measured as described above. The laminate thickness was measured in several places with a micrometer, and an average thickness calculated. The ambient temperature at which the measurements were made was recorded. On completion of these measurements, the glass content of each strip was determined by the resin burnoff method (see Section 5.4).

8.4 Experimental Results

Tables 5 and 7 give the plate curvature results. A range of plate thicknesses and glass contents was covered.

8.5 Theoretical Results

To compare the experimental results with those predicted by the Continuum Theory outlined in Section 7, the theoretical stress-free temperature was calculated for each specimen using the RARDE computer model (Ref 3).

A 1mm thick plate comprising a 0.5mm zero degree ply and a 0.5mm ninety degree ply was modelled using the basic ply properties determined in Section 6. Separate analyses were performed for fibre volume fractions of 0.5, 0.55, 0.6, 0.65 and 0.7. A temperature difference of 1°C was imposed on each laminate. Taking the predicted curvature of a 0.6 volume fraction laminate as unity, a graph of glass content normalising factor (GCNF) versus glass content was constructed (Fig 11), where

$$\text{GCNF at a } V_F \text{ of X} = \frac{\text{Predicted curvature of an X } V_F \text{ plate}}{\text{Predicted curvature of a 0.6 } V_F \text{ plate}}$$

Using the basic ply data for a 0.6 VF laminate, separate analyses were performed to establish the effect of plate thickness on predicted plate curvature. Taking the predicted curvature of a 1.0mm plate as unity, a graph of plate thickness versus thickness normalising factor (TNF) was constructed (Fig 12), where

TNF at a plate thickness Ymm = $\frac{\text{Predicted curvature of a Ymm thick plate}}{\text{Predicted curvature of a 1.0mm thick plate}}$

The RARDE model predicted the curvature for a 1mm thick plate with a glass content of 60% and an imposed thermal stress temperature of 1°C to be:

$$\chi = 2.469 \times 10^{-5} (mm^{-1})$$

The theoretical stress-free temperature was calculated for each specimen as follows, using the results of specimen 2B as an example:

Specimen 2B $V_F = 0.65$ t = 0.99mm Radius of curvature = 488.5mm

From Fig 11, GCNF = 0.85 for a $0.65V_F$ laminate

From Fig 12, TNF = 1.01 for a 0.99mm thick plate

Predicted curvature for this specimen is equal to the predicted curvature for a 1mm thick, 0.6 V_F specimen multiplied by GCNF, TNF and the difference between the test temperature and the stress-free temperature (ΔT)

ie $$\chi_{PREDICTED} = \chi_{0.6V_F, 1mm\ thick} * GCNF*TNF * \Delta T \qquad (37)$$

With the appropriate value of ΔT, $\chi_{PREDICTED} = \chi_{EXPERIMENTAL}$

Substituting into equation 37 gives:

$$\Delta T = \frac{\chi_{EXPERIMENTAL}}{\chi_{0.6V_F, 1mm\ thick} * GCNF * TNF}$$

for specimen 2B this gives:

$$\Delta T = \frac{1/488.5}{2.469 \times 10^{-5} * 0.85 * 1.01} = 96.6°C$$

Theoretical stress-free temperature (T) = ΔT + test temperature:

ie T = 96.6+22 = 118.6°C

The results of calculations using the data from the other specimens are given in Table 8.

A graph showing predicted stress-free temperature versus measured radius of curvature is given in Figure 13. A well grouped set of results was obtained, indicating a mean stress-free temperature of 119.5°C±6.1°C.

8.6 Discussion of Results

The RARDE laminate computer model predicts the residual strain behaviour of the 0°/90° asymmetric laminates accurately, provided that the stress-free temperature is taken as 119.5°C for this glass/resin system.

Defining the stress-free temperature of a laminate during the cure process is difficult since curing can be accomplished over a wide range of time/temperature combinations. Reference 15 indicates some of the possible curing schedules for the system used in this report. Gelling is carried out between 80°C and 100°C, whereas temperatures of 120°C or greater are required to develop the full mechanical properties of the resin. Although a laminate which has gelled has undergone some matrix cross-linking, it is still quite pliable and capable of being formed into a different shape prior to a full cure. Residual thermal stresses cannot exist at this stage since the matrix can flow to relieve such stresses. Raising the temperature of the laminate above the gel temperature initiates the formation of strong cross-links in the matrix, and the structure progressively stiffens until curing is complete. One would expect the stressfree temperature to be somewhere between the gel and cure conditions.

At temperatures of 100-120°C creep/stress relaxation mechanisms become significant and the basic ply transverse and shear stiffness behaviour is substantially affected. Basic ply thermal expansion coefficients are also very temperature dependent in this temperature range. Using room temperature elastic and thermal expansion constants inevitably leads to some error in modelling at the higher temperatures. A more complete model has been developed to allow for temperature dependent stiffness and thermal expansion terms (Ref 16), although the problem of defining the stress-free conditions in a laminate was not discussed.

An alternative approach to the problem is discussed by Curtis in a recent paper (Ref 17). No attempt to define a stress-free temperature or measure the temperature dependent elastic and thermal expansion coefficients was made. Curvature measurements from 0°/90° laminates taken at ambient temperature were used to calculate the lamina thermally induced strains directly. Basic ply elastic constants were determined using unidirectional tensile coupons. An assessment of the strain state in some typical aircraft lay-up configurations was then made. The advantage of this approach is that thermal expansion coefficients and a stress-free temperature are not required. Values of $(\alpha_L.\Delta T)$ and $(\alpha_T.\Delta T)$ used in equations 33 and 34 are derived from the 0°/90° curvature experiments for use in further calculations. Since α_L, α_T and ΔT cannot be defined separately by this method, the disadvantages are that the residual stress state can only be determined at one temperature (ie ambient) and only for the test material where $(\alpha_L.\Delta T)$ and $(\alpha_T.\Delta_T)$ terms have been measured. Thermal expansion coefficients and elastic constants are usually quoted in manufacturers' data for a variety of fibre/resin combinations. The RARDE model would enable an assessment of the residual stress state to be made for any such systems or combinations (hybrids) provided that a reasonable estimate of the stress-free temperature could be made for these laminates.

Manufacturers' literature for the resin system used in this report (Ref 13) indicates a heat deflection temperature (as defined by BS2782 method 102G) of 105-115°C. This test is a crude measure of the temperature at which the resin ceases to support significant loads. One would therefore expect it to be a good indication of the stress-free temperature. The predicted stress-free temperature of 119.5±6.1°C seems to support this assumption, if it is accepted that modelling with ambient temperature elastic and thermal expansion constants is not strictly accurate. Errors

due to these temperature dependent properties may not, however, be significant in the case of glass/epoxy since the increase in α_T with increasing temperature is of the same order as the decrease in E_T with increasing temperature - the thermal forces and moments (Section 7.2, equation 24) are therefore less influenced since the changes will tend to cancel each other out.

9 DESIGN IMPLICATIONS

The RARDE laminate model was used to examine the residual thermal stress state in ±θ balanced, symmetric laminates. This lay-up configuration is an approximation of the simplest winding pattern found in filament wound tubes. A 0.6 fibre volume fraction was assumed and appropriate elastic constants were chosen in accordance with Section 6.3. The stress-free temperature was taken to be 119.5°C as found experimentally in Section 8. The residual stress state was calculated for two sets of conditions, ambient and -40°C. Ambient temperature was taken as 19.5°C, which gives a stress-free temperature difference of -100°C. The stress state within each lamina in fibre (LT) axes is shown in Figure 14. The maximum residual stresses occur in ±45° laminates where the significant feature is the magnitude of the transverse tensile stress. The ultimate transverse tensile strength of a basic lamina is in the range 40-60MPa. The residual curing stress at ambient temperature is approximately 20% of this.

A temperature range of +70°C to -40°C is typical of the environmental conditions specified for military equipment. The most severe residual thermal stresses will occur in laminates at -40°C. Results of the analysis are shown in Figure 15. Transverse tensile stress in the ±45° laminates is still the main feature, exceeding 30% of the ultimate strength values.

Therefore, in the simple ±θ laminates at extremes of the temperature range for normal military equipment, residual thermal stresses exceeding 30% of the ultimate strength of the basic lamina may be expected. In the worst case a corresponding reduction in the design strength of a component would occur.

More complex lay-up configurations involving unbalanced and asymmetric laminae could lead to higher residual stresses. Temperature variations within a component and thermal shock, though not the subject of this report, are additional causes of stress. Hybrid structures fabricated from layers of one material (eg GRP) combined with layers of another material (eg Kevlar) can induce large residual stresses in the laminae. An example of this is given in Reference 1 where the laminate model was used to analyse a glass/Kevlar hybrid comprising laminae oriented (0°/0°/+55°/-55°/+55°/-55°). The 0° laminae were Kevlar/epoxy and the ±55° laminae were glass/epoxy. At ambient temperature transverse tensile stresses in the Kevlar/epoxy laminae approach 70% of their ultimate value.

Recent work by Curtis (Ref 15) indicates that moisture absorption by a composite leads to relief of the residual curing stresses. The rate at which this will occur depends upon many factors such as the thickness of the laminate, the ambient moisture conditions and the moisture diffusion coefficient of the resin systems. Although this effect can be beneficial

to a component during its Service life, until recognised stress relieving processes for composites are developed and applied to components before they enter Service, the designer must assume that the full effect of curing stress will be present.

10 CONCLUSIONS

1) From the limited amount of modelling carried out in this report it can be seen that residual curing stresses can significantly affect the performance of fibre reinforced composite components. Therefore in the majority of cases some attempt to estimate their magnitude at the component design stage is necessary.

2) Evidence in this report based on glass/epoxy composites indicates that the RARDE laminate model can be used successfully for this purpose provided that relevant lamina elastic and thermal properties are available.

3) If heat deflection temperature information can be obtained for a proposed resin system, it can be used as a reasonable estimate of the stress-free temperature for modelling.

4) For other fibre/matrix combinations where elastic and thermal expansion properties are more highly temperature dependent a more exact incremental model may be required. It may be simpler in these cases to establish a stress-free temperature by experiment on 0°/90° laminated plates.

11 REFERENCES

1	Hinton M J	The Elastic Properties of Filament Wound Glass-Reinforced Plastic Tubes, RARDE Technical Report 14/79
2	Calcote Lee R	The Analysis of Laminated Composite Structures, Van Nostrand Reinhold Co, 1969
3	Hinton M J	A General Model for Predicting the Mechanical Properties of Fibre Reinforced Plastic Laminates under Complex Loading, RARDE Technical Report 17/80
4	Cawthorne D & Hinton M J	Internal Pressurization of Filament Wound Glass Fibre Reinforced Epoxy Resin Tubes, RARDE Technical Report 14/76
5	Brown E	The Effect of a Two-Stage Curing Schedule on the Fibre Loading and Transparency of Unidirectionally Wound Glass Fibre/Epoxy Resin Plates, AERE Report No R8161
6	Cawthorne D & Hinton M J	Filament Winding: Operation of Baer Machine and Materials Choice, RARDE Unpublished Report.

7	Hinton M J	Measurement of the Thermal Expansion Coefficient of Filament Wound Glass Fibre Reinforced Epoxy Resin Tubes using a Strain Gauge Technique, RARDE Unpublished Report.
8	Kelly A	Strong Solids, Oxford University Press
9	Tsai S W	Structural Behaviour of Composite Materials, NASA CR-71, July 1964.
10	Broutman L T & Krock R H	Modern Composite Materials. Addison-Wesley Publishing Co, 1967
11	Brannan R T	J Am Ceram Soc, 36, 1953, pp 230-231
12	Kroenke W J	Anisotropic Glass Fibres and Property-Composition Relationships, Airforce Materials Laboratory Technical Report No AFML-TR-65-189, 1965
13	Wilson A	Silenka UK Ltd, private communication.
14	Manders P W & Bader M G	Simulated Impact Damage in Filament Wound Glass Fibre Reinforced Tubes, University of Surrey, MOD Contract No 2064/043 Mat R Third Report, June 1980
15		Araldite MY750 with Hardener HY917 and Accelerator DY063, Ciba-Geigy (UK) Ltd Instruction Sheet No C35b, February 1975
16	Hahn H T & Pagano N J	Curing Stresses in Composite Laminates J Composite Materials, 9, 1975, p91
17	Curtis P T	Residual Strains and the Effects of Moisture in Fibre Reinforced Laminates, RAE Tech Report 80045, April 1980

Reports quoted are not necessarily available to members of the public or to commercial organisations.

12 LIST OF SYMBOLS

ε	Strain
γ	Shear Strain
σ	Stress
τ	Shear Stress
E	Young's Modulus
G	Shear Modulus
μ	Poisson's Ratio
LT	Coordinate axes based on lamina principle fibre direction
XY	Arbitrary coordinate system at angle $\theta°$ to LT coordinate system
$\theta°$	Ply angle, ie the angle through which the XY axes are rotated relative to the LT axes
[]	Matrix
α	Linear coefficient of thermal expansion
T	Temperature

TABLE 1 Longitudinal Tensile Specimen Results

GLASS VOLUME FRACTION V_F	E_L GPa	μ_{LT}	α_L STRAIN/°C	α_T STRAIN/°C
0.51	37.81	0.261	9.13	31.73
0.525	39.96	0.276	10.19	31.79
0.54	39.17	0.290	9.48	35.10
0.57	43.84	0.165	9.67	32.25
0.585	45.10	0.348	8.85	32.83
0.60	45.10	0.311	8.22	24.97
0.605	44.88	0.290	8.15	24.32
0.62	46.97	0.266	7.87	23.93
0.62	47.06	0.296	8.55	26.40
0.625	47.19	0.283	7.68	25.10
0.72	53.91	0.266	BROKEN STRAIN GAUGE	

TABLE 2 Transverse Tensile Specimen Results

GLASS VOLUME FRACTION V_F	E_T GPa	μ_{TL}	α_L STRAIN/°C	α_T STRAIN/°C
0.53	13.1	0.088	11.56	33.15
0.54	13.92	0.087	9.48	28.87
0.56	13.79	0.080	8.94	26.53
0.575	13.60	0.086	9.43	29.52
0.59	BROKEN STRAIN GAUGE		9.59	27.57
0.60	15.31	0.105	7.21	24.39
0.615	16.91	0.101	8.85	27.77
0.625	16.40	0.090	8.18	25.62
0.70	21.53	0.081	7.06	18.84

TABLE 3 Predicted Elastic Properties of Unidirectional Laminae

GLASS VOLUME FRACTION V_F	E_L GPa MODIFIED LAW OF MIXTURES	E_T GPa TSAI C=0.4	E_T GPa TSAI C=0.5	μ_{LT} LAW OF MIXTURES	μ_{TL}(C=0.4) RECIPROCAL THEOREM	μ_{TL}(C=0.5) RECIPROCAL THEOREM
0.50	38.72	11.61	12.60	0.29	0.087	0.094
0.55	42.15	13.08	14.28	0.283	0.088	0.096
0.60	45.58	14.90	16.23	0.278	0.090	0.099
0.65	49.01	16.99	18.51	0.271	0.094	0.102
0.70	52.43	19.43	21.21	0.266	0.099	0.108

TABLE 4 Predicted Thermal Expansion Coefficients of Unidirectional Laminae

GLASS VOLUME FRACTION V_F	α_L STRAIN/°C	α_T STRAIN/°C
0.50	7.25	31.7
0.55	6.84	29.02
0.60	6.49	26.34
0.65	6.19	23.66
0.70	5.93	20.98

TABLE 5 Torsional Shear Test Results

TUBE NO	WALL THICKNESS (mm)	TORQUE AT FAILURE (Nm)	STRAIN AT FAILURE (%)	SHEAR STRESS AT FAILURE (MPa)	SECANT MODULUS AT FAILURE (GPa)	GLASS VOLUME FRACTION V_F
729A	1.12	368	3.68	74.4	2.02	0.61
B	"	380	3.84	76.9	2.00	0.60
C	"	378	4.16	76.5	1.84	0.61
F	"	383	3.55	77.5	2.18	0.59
H	"	350	4.17	70.8	1.70	0.62
N	"	383	3.94	77.5	1.97	0.62
P	"	356	2.56	72.0	2.81	0.61
R	"	358	4.94	72.4	1.47	0.61
W	"	395	4.28	79.9	1.87	0.59
X	"	344	3.89	69.6	1.79	0.62
Y	"	340	2.33	68.8	2.95	0.62
		AVERAGE	3.76	74.2	2.05	0.61
		C OF V	20%	5%	22%	2%

TABLE 6 Plate Curvature Results, 0°/0°/90°/90° Plates, 22°C

SPECIMEN NO	GLASS VOLUME FRACTION	PLATE THICKNESS (mm)	RADIUS OF CURVATURE (mm)
2B	0.65	0.99	488.5
2C	0.66	1.00	482.5
2D	0.655	1.03	514.2
2E	0.65	1.05	517.6
2F	0.65	1.08	521.0
2G	0.65	1.10	539.0
6A	0.61	1.09	443.7
6B	0.61	1.14	443.7
6C	0.61	1.16	443.7
6D	0.605	1.18	440.2
6E	0.60	1.21	452.9
6F	0.585	1.22	456.7
6G	0.57	1.22	451.1
6H	0.57	1.19	440.2
18B	0.575	1.07	447.5
18C	0.58	1.07	451.8
18D	0.615	1.07	470
18E	0.65	1.07	505.9
18F	0.64	1.07	535
18G	0.63	1.07	535
18H	0.63	1.05	495

TABLE 7 Plate Curvature Results, 0°/90° Plates, 22°C

SPECIMEN NO	GLASS VOLUME FRACTION	PLATE THICKNESS (mm)	RADIUS OF CURVATURE (mm)
3B	0.605	0.74	312.5
3C	0.59	0.71	298.9
3D	0.595	0.71	297.1
3E	0.60	0.71	291.8
3F	0.61	0.69	294.4
3G	0.62	0.70	296.0
13A	0.65	0.58	314.3
13B	0.655	0.60	266.7
13C	0.66	0.60	288.3
13D	0.655	0.61	288.3
13E	0.65	0.61	290.1
13F	0.645	0.61	287.5
13G	0.64	0.61	281.7
13H	0.64	0.58	279.3
15B	0.60	0.74	322.4
15C	0.58	0.69	306.0
15D	0.595	0.66	289 8
15E	0.61	0.64	296.1
15F	0.61	0.66	297.1
15G	0.61	0.66	306
15H	0.61	0.67	307.8

TABLE 8 Theoretical Stress-Free Temperature Pradiction

SPECIMEN NO	STRESS-FREE TEMPERATURE	SPECIMEN NO	STRESS-FREE TEMPERATURE	SPECIMEN NO	STRESS-FREE TEMPERATURE
2B	118.6	6A	124.9	18B	111.8
2C	122.2	6B	129.6	18C	112.2
2D	119.1	6C	130.7	18D	118.2
2E	119.1	6D	132.4	18E	122.5
2F	120.8	6E	129.9	18F	113.7
2G	119.7	6F	125.5	18G	110.7
		6G	122.4	18H	116.7
		6H	122.8		

SPECIMEN NO	STRESS-FREE TEMPERATURE	SPECIMEN NO	STRESS-FREE TEMPERATURE	SPECIMEN NO	STRESS-FREE TEMPERATURE
3B	119	13A	110.6	15B	114.5
3C	114.7	13B	130.7	15C	107.6
3D	117.4	13C	124.2	15D	112.8
3E	120.8	13D	124.6	15E	111.6
3F	119.2	13E	122.1	15F	114.8
3G	123.7	13F	121.3	15G	112.1
		13G	121.6	15H	113.4
		13H	118.2		

MEAN STRESS-FREE TEMPERATURE = 119.5°C

STANDARD DEVIATION = 6.1°C

COEFFICIENT OF VARIATION = 5.1%

FIG. 1

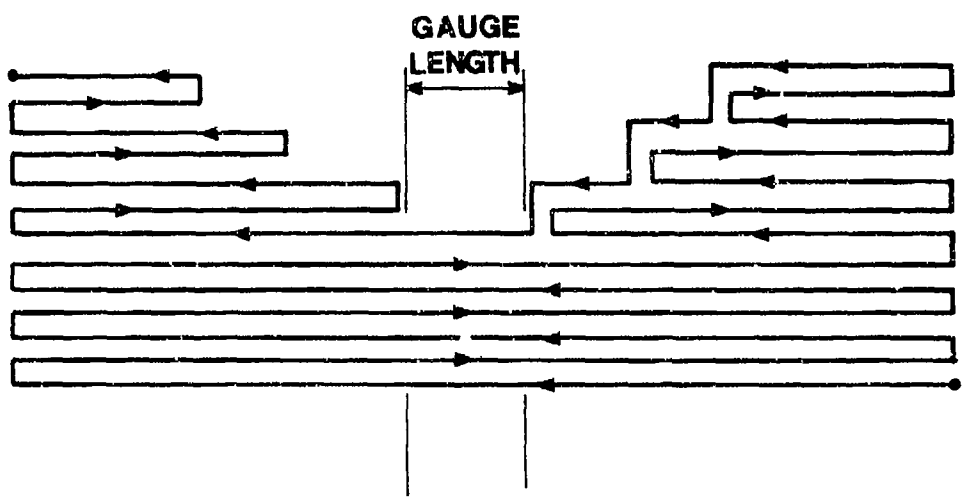

FIG.1 SCHEMATIC WINDING PATTERN SHOWING END BUILD UPS

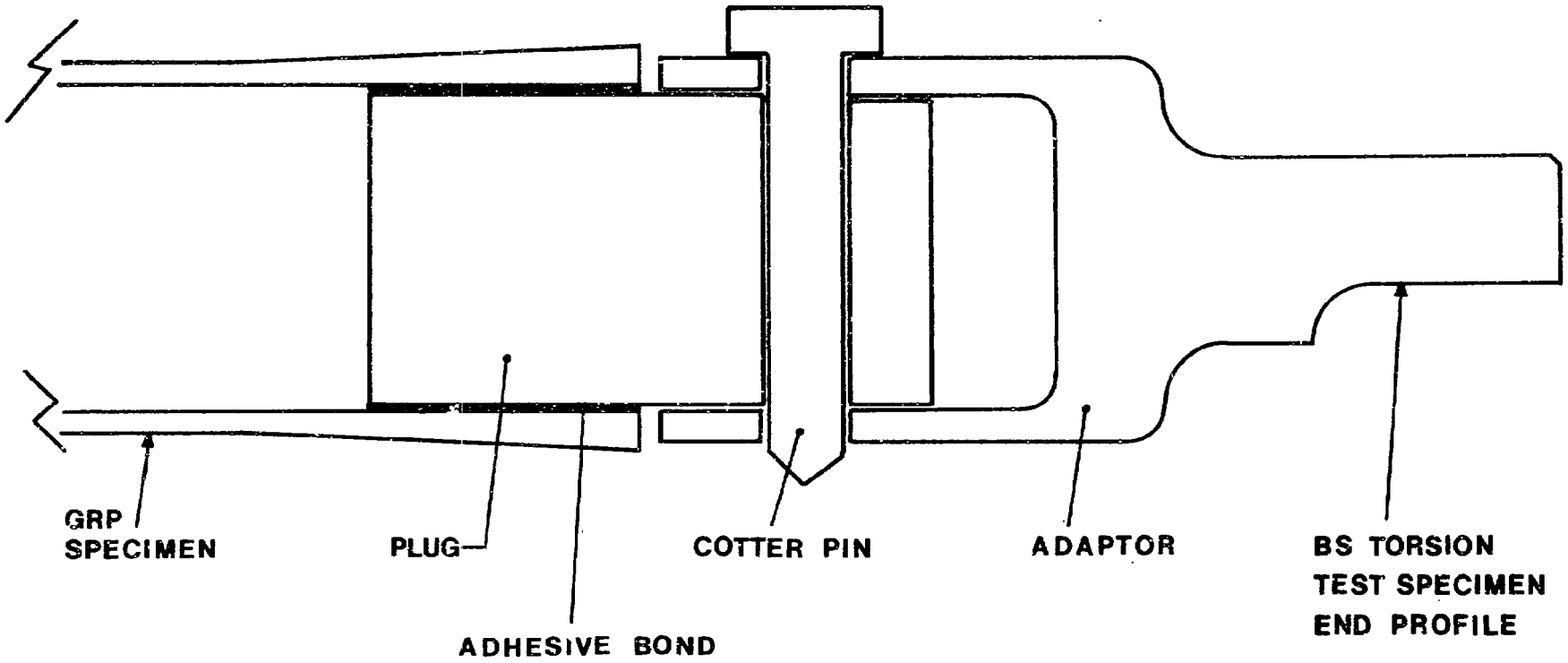

FIG. 2 TORSION TEST ADAPTOR ASSEMBLY

FIG. 2

FIG. 3

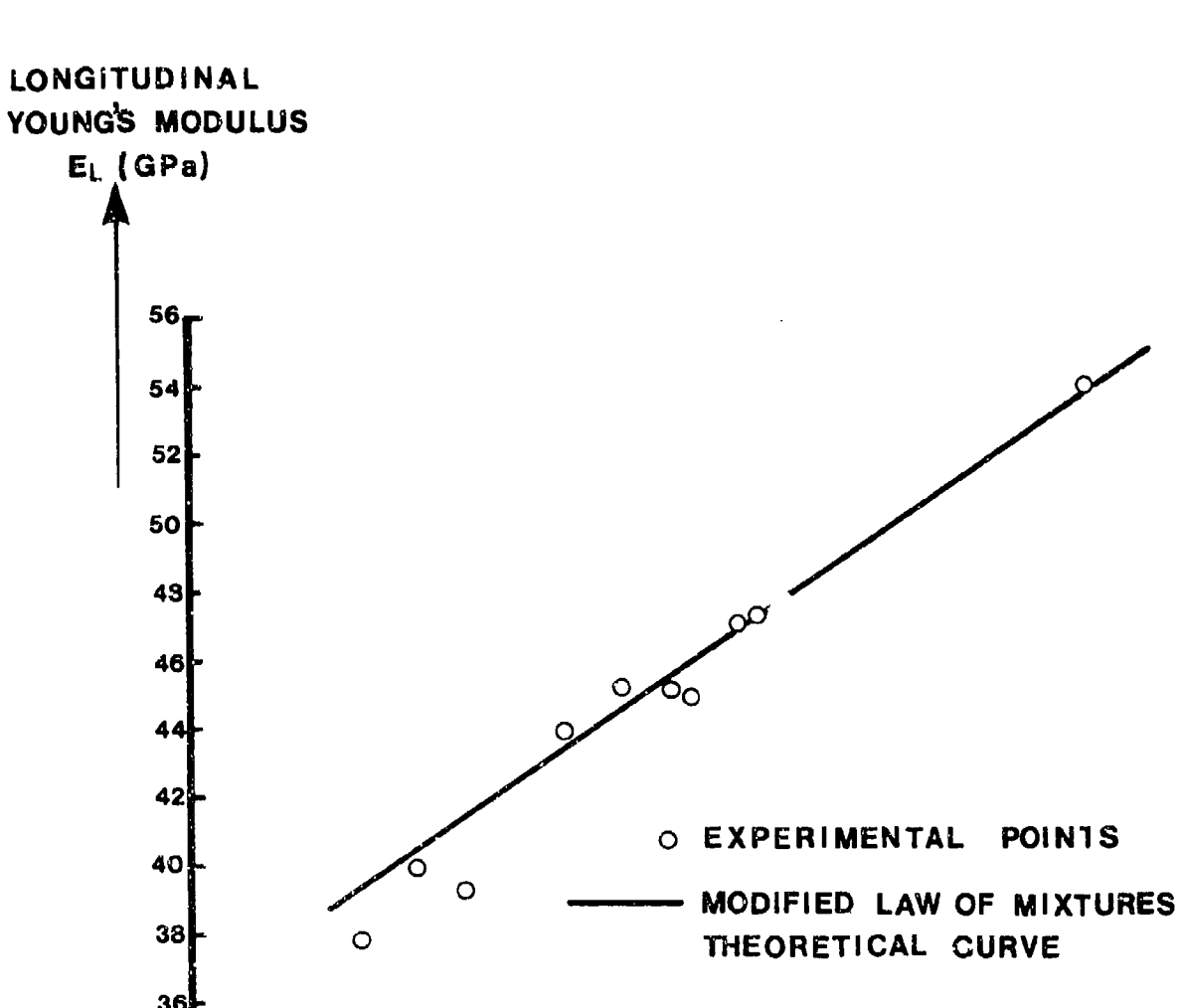

FIG. 3 LONGITUDINAL YOUNG'S MODULUS vs GLASS VOLUME FRACTION FLAT UNIDIRECTIONAL BASIC LAMINA

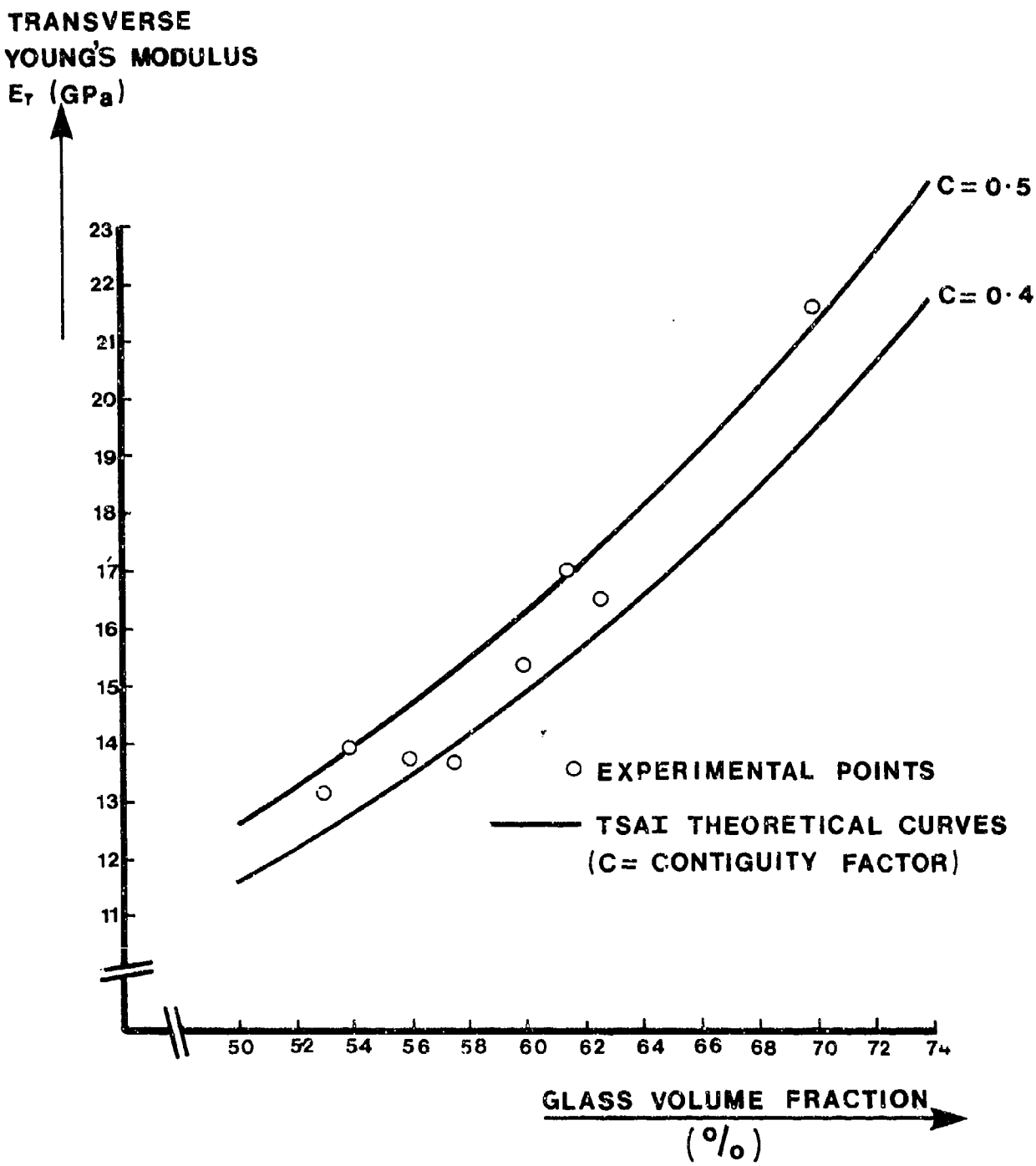

FIG. 4 TRANSVERSE YOUNG'S MODULUS vs GLASS VOLUME FRACTION FLAT UNIDIRECTIONAL BASIC LAMINA

FIG. 5

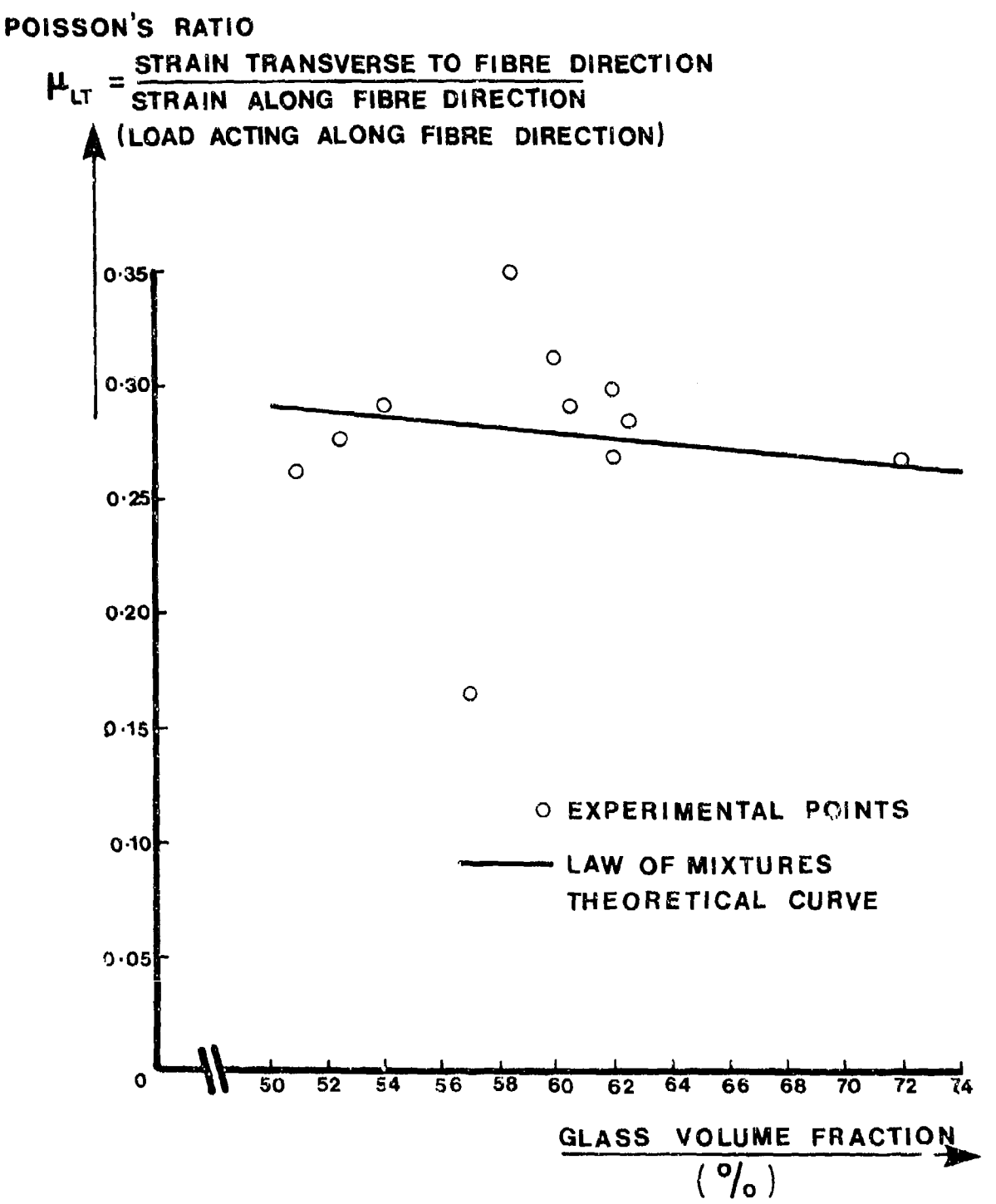

FIG. 5 POISSON'S RATIO vs GLASS VOLUME FRACTION
FLAT UNIDIRECTIONAL BASIC LAMINA

FIG. 6

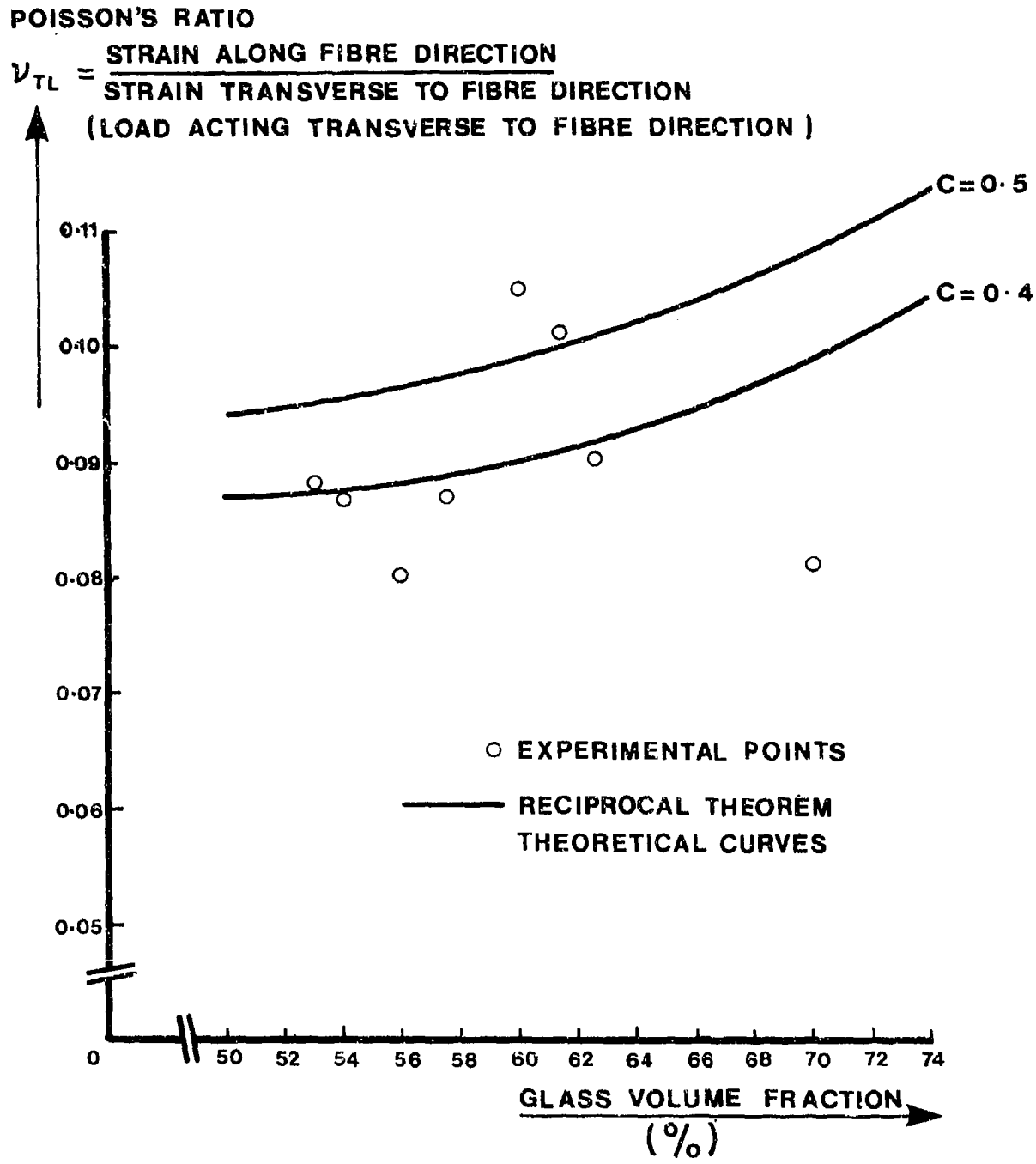

FIG.6 POISSON'S RATIO vs GLASS VOLUME FRACTION FLAT UNIDIRECTIONAL BASIC LAMINA

FIG. 7

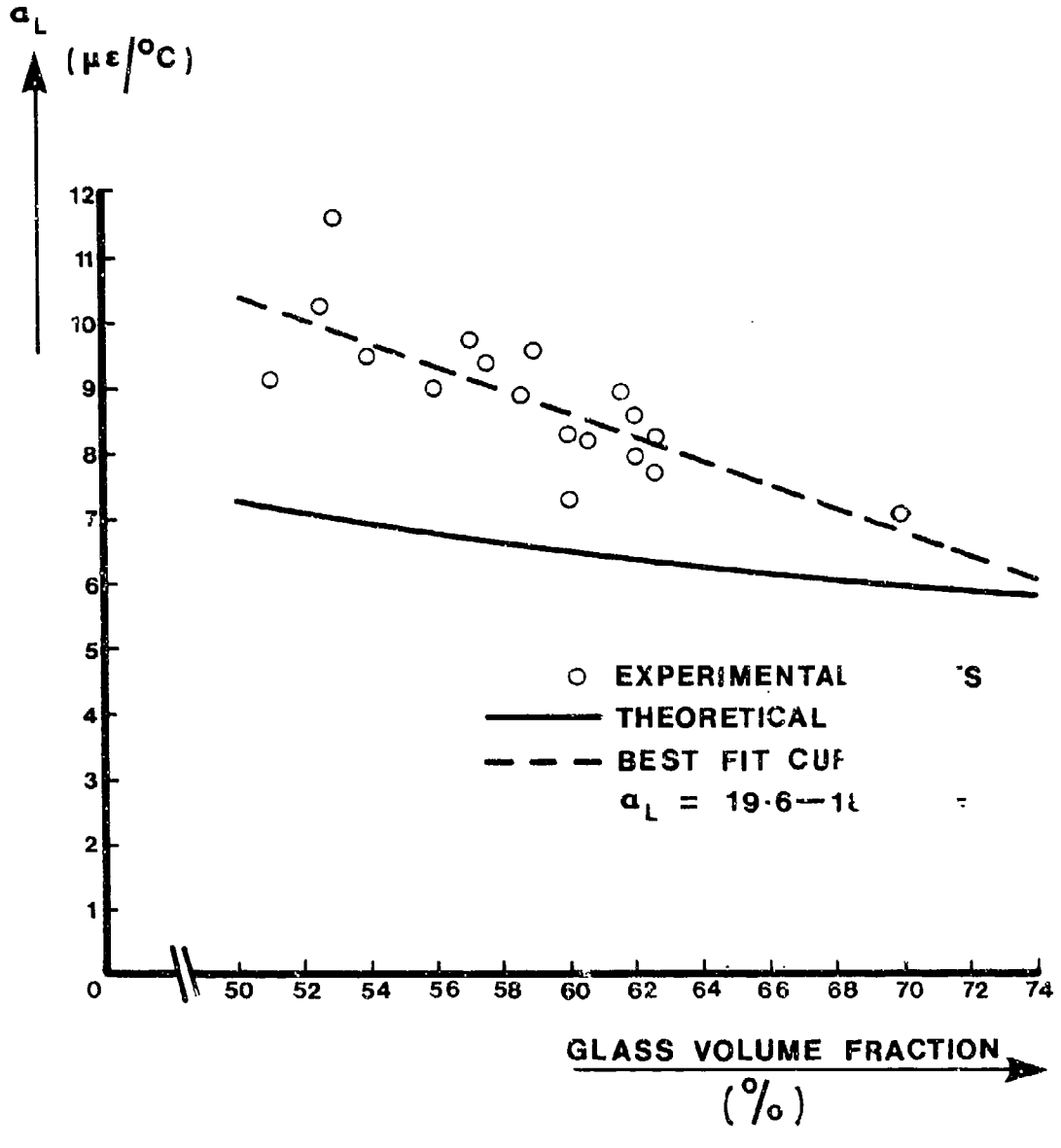

FIG. 7 LONGITUDINAL THERMAL EXPANSION COEFFICIENT vs GLASS VOLUME FRACTION FLAT UNIDIRECTIONAL BASIC LAMINA

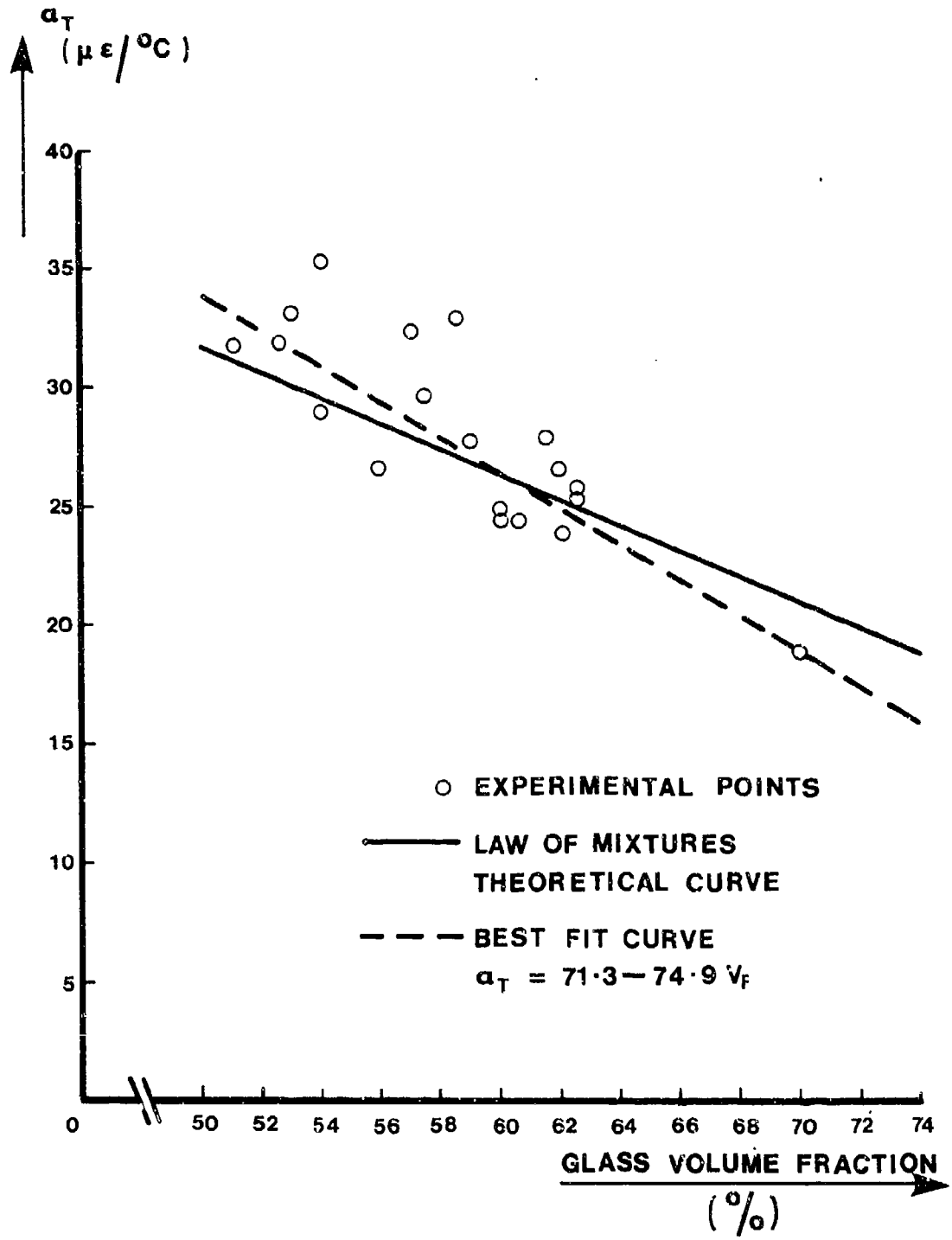

FIG. 8 TRANSVERSE THERMAL EXPANSION COEFFICIENT vs GLASS VOLUME FRACTION FLAT UNIDIRECTIONAL BASIC LAMINA

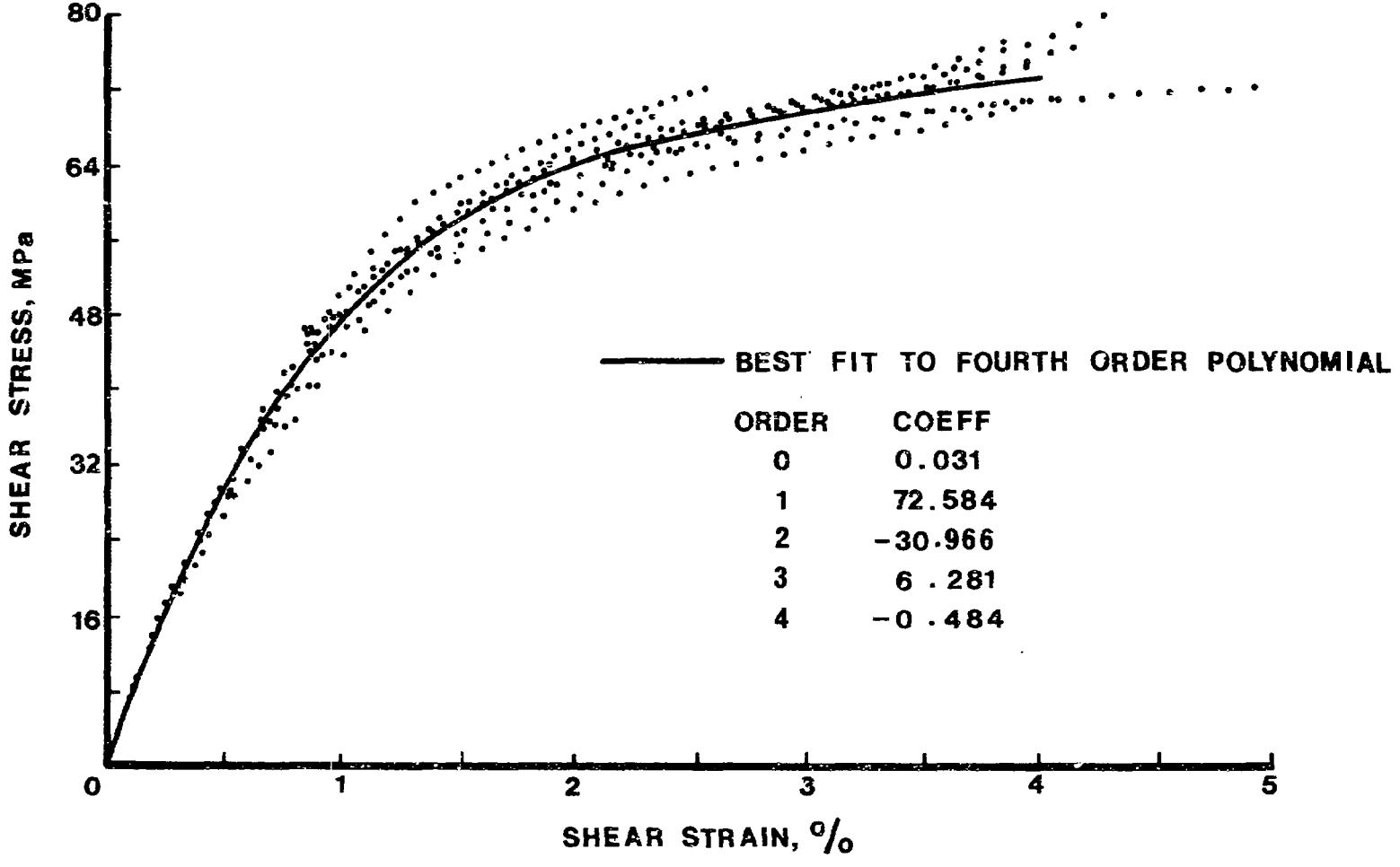

FIG.9 SHEAR STRAIN vs SHEAR STRESS FOR A UNIDIRECTIONAL GRP LAMINATE

FIG. 9

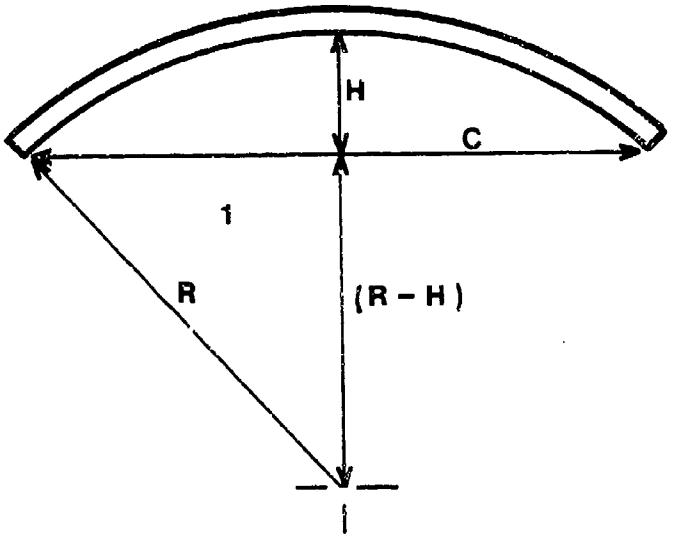

FOR TRIANGLE 1 :– $R^2 = (R-H)^2 + (\frac{C}{2})^2$

$$R^2 = R^2 - 2RH + H^2 + (\frac{C}{2})^2$$

$$2RH = H^2 + (\frac{C}{2})^2$$

$$R = \frac{(\frac{C}{2})^2 + H^2}{2H}$$

MEASURE :–

1. C WITH A RULER
2. H WITH A DEPTH GAUGE WHILST PLATE IS ON A FLAT SURFACE
3. TEMPERATURE AT WHICH MEASUREMENTS ARE MADE

FIG.10 METHOD OF MEASURING PLATE RADIUS OF CURVATURE

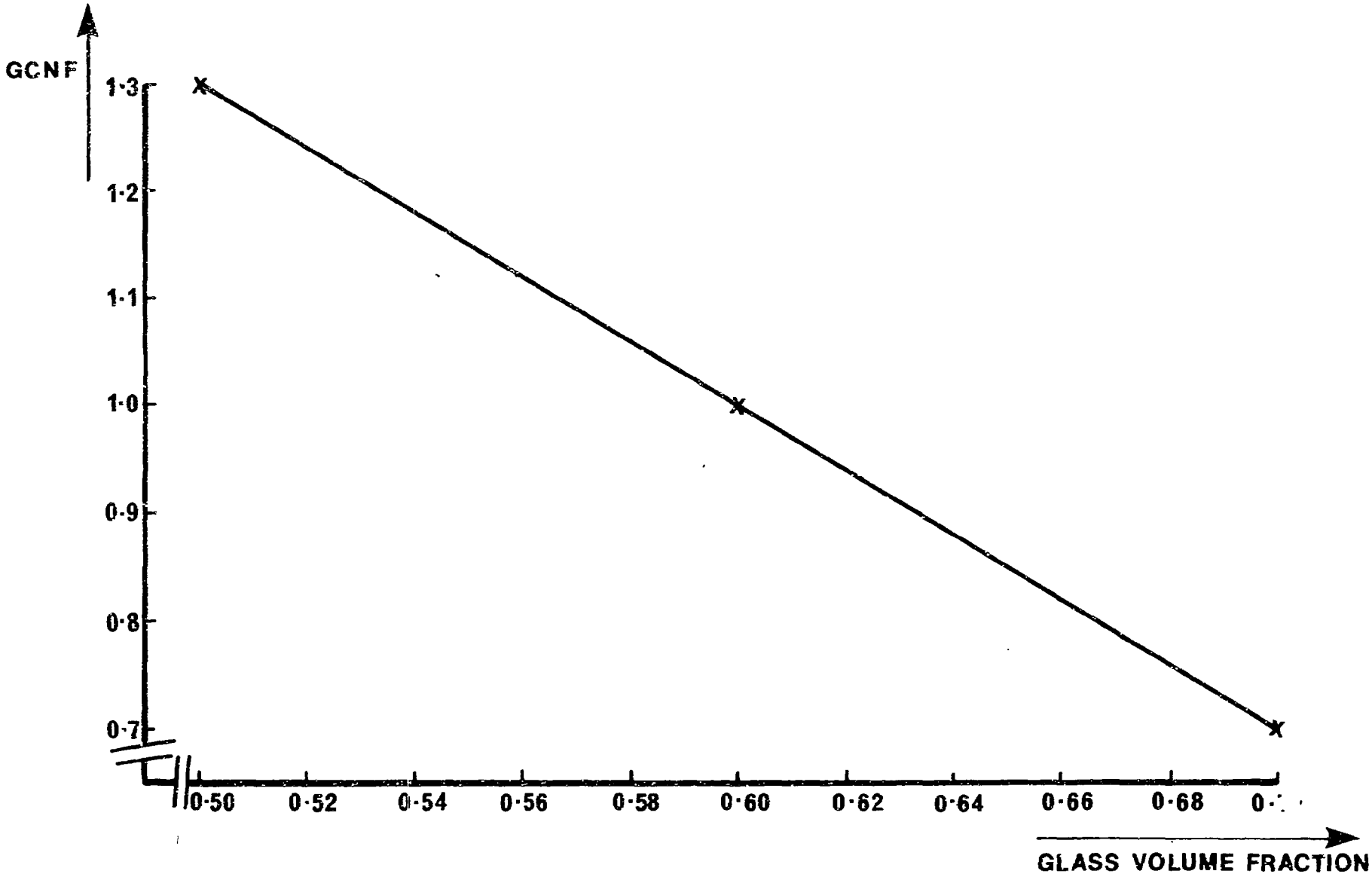

FIG. 11 GLASS CONTENT NORMALIZING FACTOR vs GLASS VOLUME FRACTION

FIG. 11

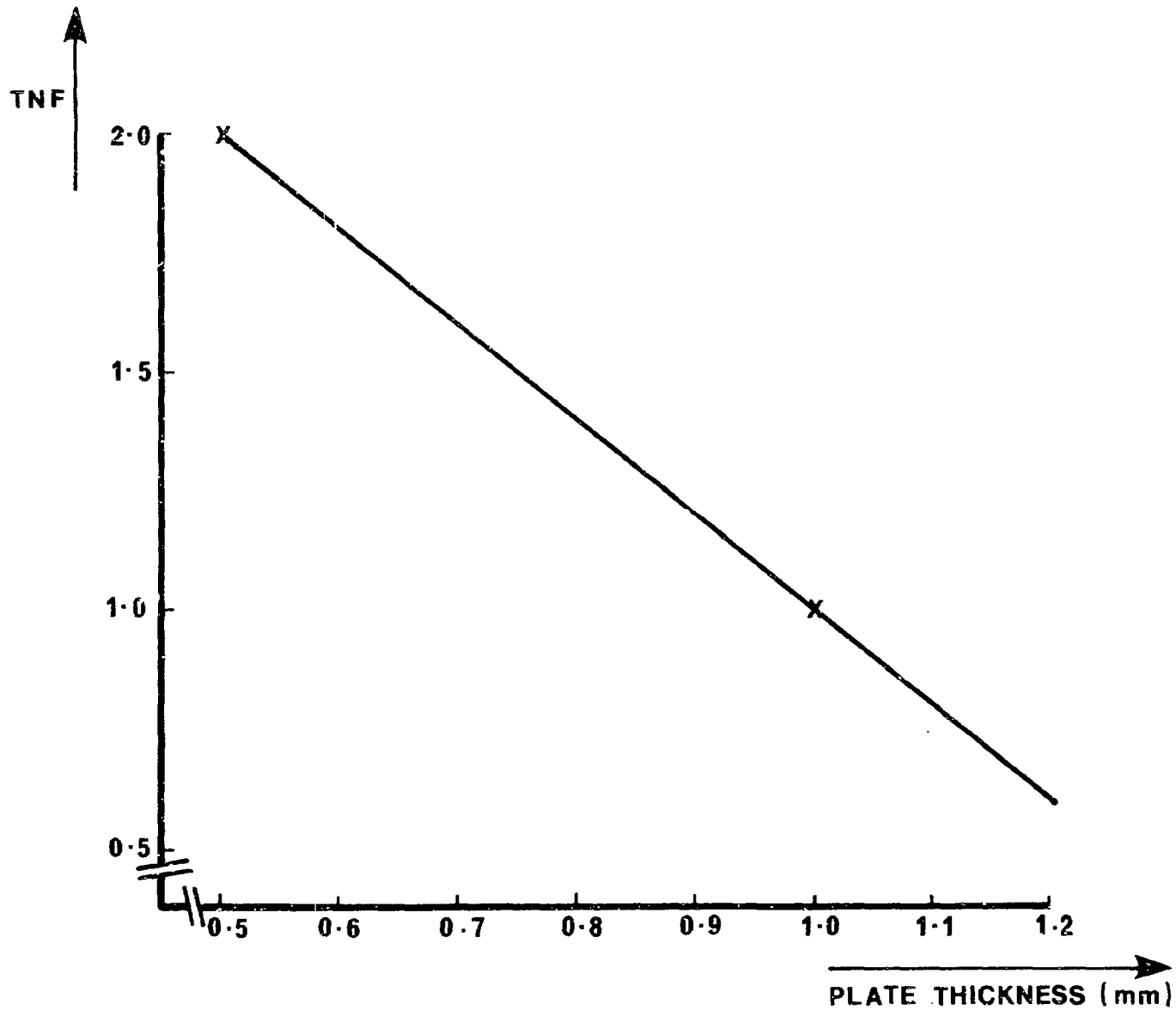

FIG.12 THICKNESS NORMALIZING FACTOR vs PLATE THICKNESS

FIG. 12

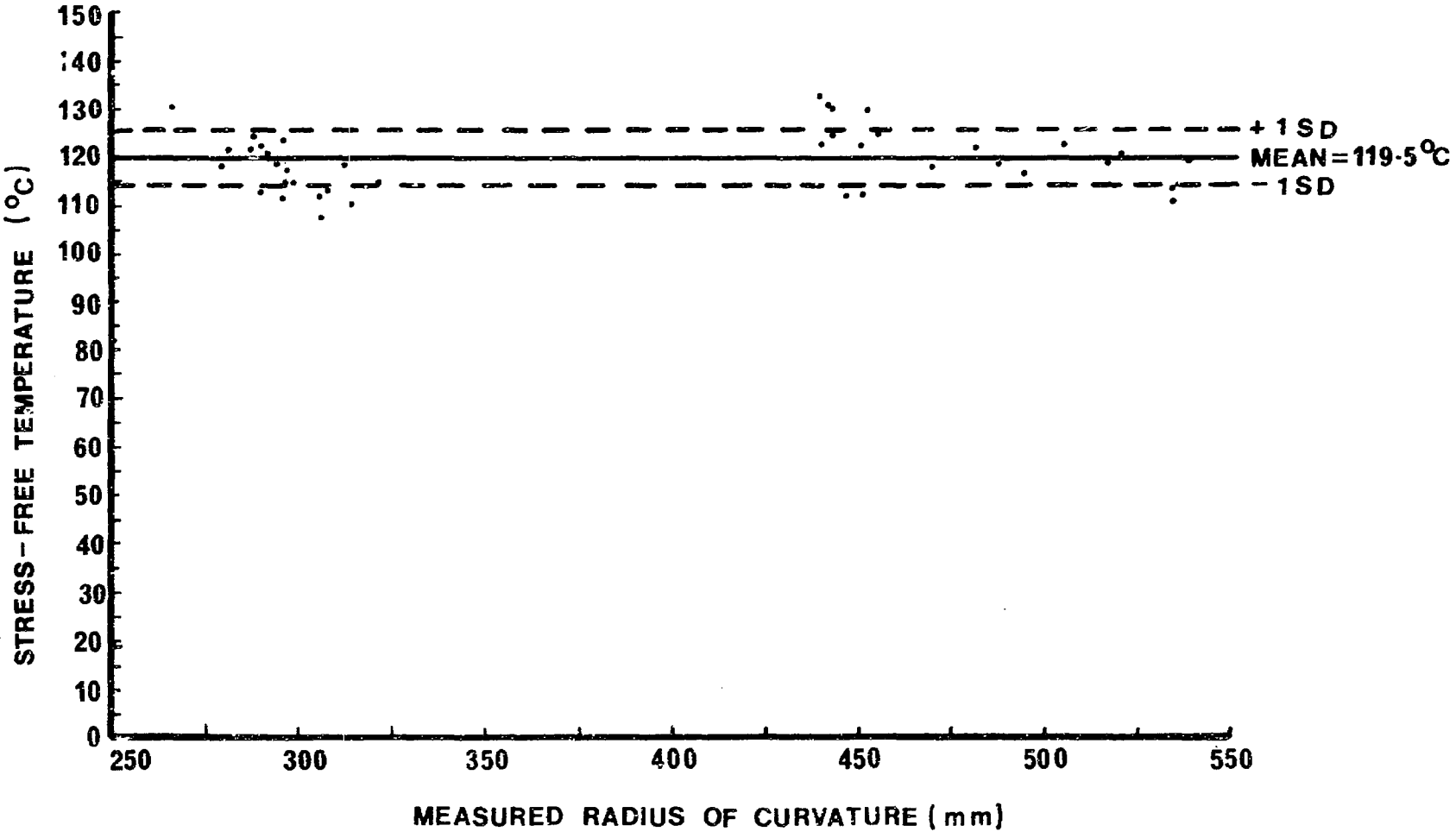

FIG.13 PREDICTION OF STRESS-FREE TEMPERATURE

FIG.13

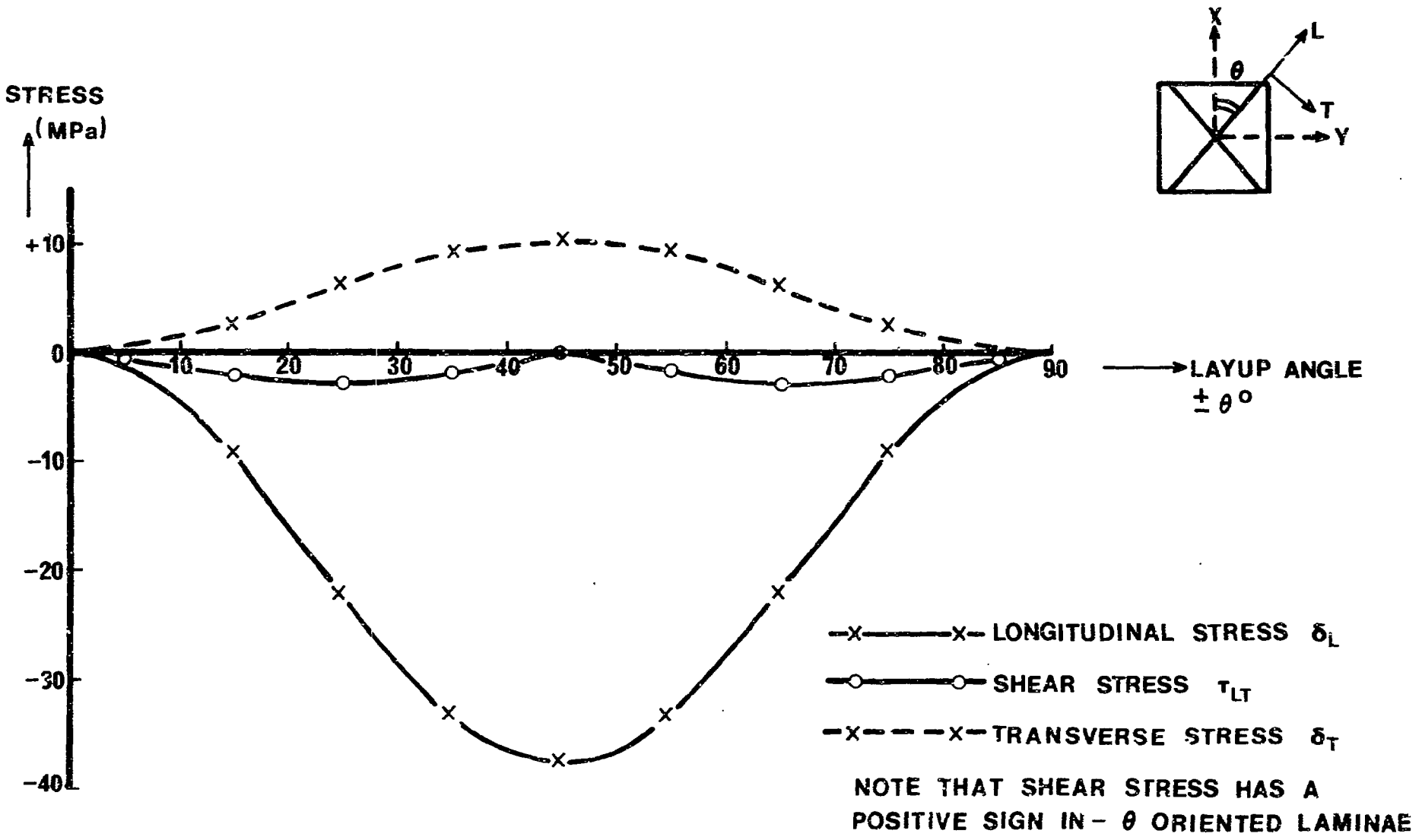

FIG. 14 RESIDUAL STRESSES IN ± θ° BALANCED, SYMMETRIC GLASS / EPOXY LAMINATES AT AMBIENT TEMPERATURE (ΔT = 100° C)

FIG. 14

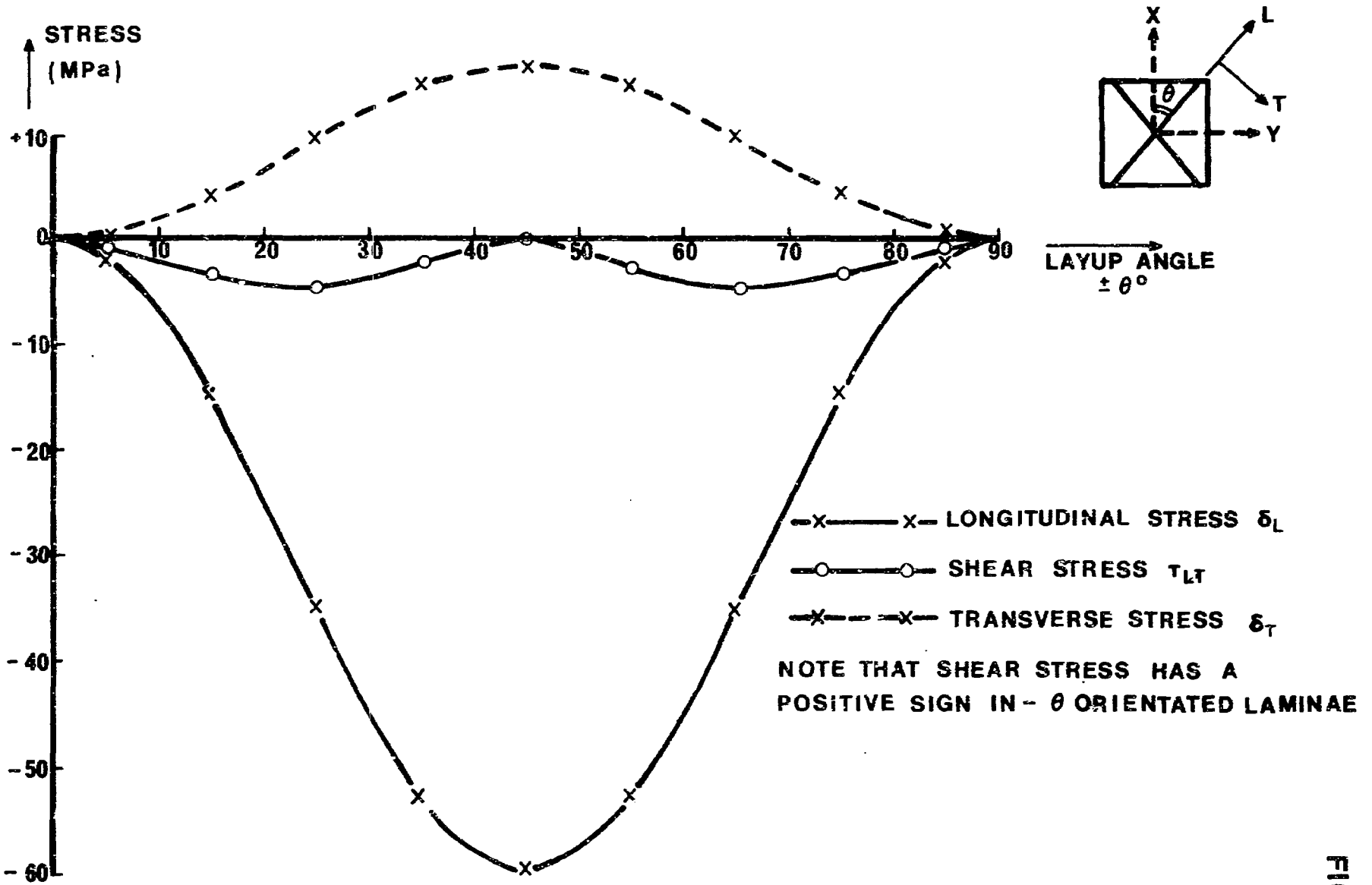

FIG. 15 RESIDUAL STRESSES IN ± θ° BALANCED, SYMMETRIC GLASS / EPOXY LAMINATES AT -40°C (ΔT = 160°C)

FIG. 15

DOCUMENT CONTROL SHEET

(Notes on completion overleaf)

Overall security classification of sheet ..... UNLIMITED .....

(As far as possible this sheet should contain only unclassified information. If is is necessary to enter classified information, the box concerned must be marked to indicate the classification eg (R),(C) or (S)).

1. DRIC Reference (if known)	2. Originator's Reference RARDE Report 4/82	3. Agency Reference	4. Report Security Classification UNLIMITED
5. Originator's Code (if known) 851600	6. Originator (Corporate Author) Name and Location **Ministry of Defence** **Royal Armament Research and Development Establishment**		
5a. Sponsoring Agency's Code (if known)	6a. Sponsoring Agency (Contract Authority) Name and Location		

7. Title
Investigation of Residual Stresses in a Hot Cured Glass Fibre Reinforced Epoxy Resin Composite

7a. Title in Foreign Language (in the case of translations)

7b. Presented at (for conference papers). Title, place and date of conference

8. Author 1. Surname, initials	9a Author 2	9b Authors 3, 4...	10. Date	pp	ref
Hinton M J			April 1982	43	17
11. Contract Number	12. Period	13. Project	14. Other References		

15. Distribution statement
No limitations

Descriptors (or keywords)
Residual stresses **Epoxy resin**
Laminate theory
Curing stress
Fibre reinforced composites
Glass fibre

continue on separate piece of paper if necessary

Abstract **Basic lamina elastic constants and thermal expansion coefficients have been determined for an 'E' glass fibre reinforced epoxy resin system over a range of fibre contents. These have been used as input data to a theoretical model which predicts laminate residual strains and stresses. Residual strains have also been measured experimentally. Theory and experiment were in good agreement indicating a stress-free temperature comparable to the heat deflection temperature of the resin. It is shown that in some cases residual stresses can be significant percentages of the ultimate strength of the lamina and must be allowed for in design.**

UNLIMITED

Ministry of Defence | 678.029.4-419
Royal Armament Research and Development Establishment | 666.189.2
RARDE Report 4/82 | 620.172.21

Investigation of Residual Stresses in a Hot Cured Glass Fibre Reinforced Epoxy Resin Composite

M J Hinton — April 1982

Basic lamina elastic constants and thermal expansion coefficients have been determined for an 'E' glass fibre reinforced epoxy resin system over a range of fibre contents. These have been used as input data to a theoretical model which predicts laminate residual strains and stresses. Residual strains have also been measured experimentally. Theory and experiment were in good agreement indicating a stress-free temperature comparable to the heat deflection temperature of the resin. It is shown that in some cases residual stresses can be significant percentages of the ultimate strength of the lamina and must be allowed for in design.

22pp 8tabs 15figs 17refs UNLIMITED

UNLIMITED

Ministry of Defence | 678.029.4-419
Royal Armament Research and Development Establishment | 666.189.2
RARDE Report 4/82 | 620.172.21

Investigation of Residual Stresses in a Hot Cured Glass Fibre Reinforced Epoxy Resin Composite

M J Hinton — April 1982

Basic lamina elastic constants and thermal expansion coefficients have been determined for an 'E' glass fibre reinforced epoxy resin system over a range of fibre contents. These have been used as input data to a theoretical model which predicts laminate residual strains and stresses. Residual strains have also been measured experimentally. Theory and experiment were in good agreement indicating a stress-free temperature comparable to the heat deflection temperature of the resin. It is shown that in some cases residual stresses can be significant percentages of the ultimate strength of the lamina and must be allowed for in design

22pp 8tabs 15figs 17refs UNLIMITED

UNLIMITED

Ministry of Defence | 678.029.4-419
Royal Armament Research and Development Establishment | 666.189.2
RARDE Report 4/82 | 620.172.21

Investigation of Residual Stresses in a Hot Cured Glass Fibre Reinforced Epoxy Resin Composite

M J Hinton — April 1982

Basic lamina elastic constants and thermal expansion coefficients have been determined for an 'E' glass fibre reinforced epoxy resin system over a range of fibre contents. These have been used as input data to a theoretical model which predicts laminate residual strains and stresses. Residual strains have also been measured experimentally. Theory and experiment were in good agreement indicating a stress-free temperature comparable to the heat deflection temperature of the resin. It is shown that in some cases residual stresses can be significant percentages of the ultimate strength of the lamina and must be allowed for in design.

22pp 8tabs 15figs 17 refs UNLIMITED

UNLIMITED

Ministry of Defence | 678.029.4-419
Royal Armament Research and Development Establishment | 666.189.2
RARDE Report 4/82 | 620.172.21

Investigation of Residual Stresses in a Hot Cured Glass Fibre Reinforced Epoxy Resin Composite

M J Hinton — April 1982

Basic lamina elastic constants and thermal expansion coefficients have been determined for an 'E' glass fibre reinforced epoxy resin system over a range of fibre contents. These have been used as input data to a theoretical model which predicts laminate residual strains and stresses. Residual strains have also been measured experimentally. Theory and experiment were in good agreement indicating a stress-free temperature comparable to the heat deflection temperature of the resin. It is shown that in some cases residual stresses can be significant percentages of the ultimate strength of the lamina and must be allowed for in design.

22pp 8tabs 15figs 17refs UNLIMITED